

## FUNDAMENTALS

Many industrial processes involve the transfer and feeding of bulk solids, and the ability of such materials to flow in a controlled manner during these operations is critical to product quality. Hoppers, bin, and silos are used to store granular raw materials, intermediates, and final products. With modifications, they can also be used as process vessels, such as purge columns, heaters and coolers, and moving bed reactors. Transfer chutes are inclined or vertical assemblies in which bulk solids flow by gravity from one location to another. Unlike hoppers, bins, or silos, chutes are not filled with the bulk material.

Bulk solids have unique properties that cause them to flow differently from liquids. Bulk solids are frictional and in general are compressible. Liquids are frictionless and are nearly incompressible. Bulk solid flow properties are strongly dependent on the consolidation stresses applied and minimally if at all dependent on strain rate, whereas fluid flow properties are strongly dependent on strain rate and minimally dependent on absolute pressure. In addition, bulk solids are anisotropic whereas liquids are isotropic.

### Definitions

When discussing storage and handling of granular materials, the following definitions are commonly accepted:

*Bulk solid* – a material consisting of discrete solid particles, handled in bulk form.

*Hopper, bin, or silo* – storage vessels for bulk solids. The terms are often used interchangeably. Silos usually refer to tall vessels that store several tons of material. Hoppers and bins frequently refer to smaller vessels. The converging section of a storage vessel is often called the hopper section. Examples of hopper, bin, and silo geometries are given in Figure 1. For simplicity, the term *bin* will be used henceforth as a descriptor for a storage vessel of any size.

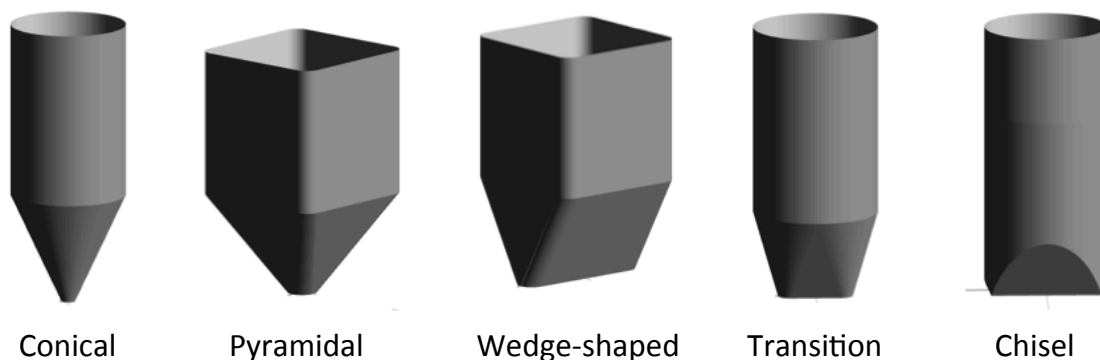


**Figure 1. Common bin geometries.**

*Chute* – equipment used to transfer bulk material by gravity between other pieces of equipment. The cross-section must be only partially full of material; otherwise it acts as a sloping bin or hopper.

*Cylinder* – vertical part of a bin. The cylinder may be round or rectangular and has a constant cross section.

*Expanded flow* – flow pattern inside a bin, where all the bulk material is in motion in the bottom portion of the vessel when withdrawn, but flow only occurs in a flow channel in the top portion of the vessel centered over the outlet.

*Feeder* – device for modulating the withdrawal rate of bulk material, *e.g.*, rotary valves, screw feeders, and belt feeders. Often, a valve or gate is used to stop and start flow, but such devices in general should not be used to control the discharge rate of bulk solids.

*Flow channel* – the space in a bin in which the bulk solid is actually flowing at any point in time during withdrawal.

*Funnel flow* – flow pattern inside a bin, where the bulk material only moves in a flow channel above the outlet when withdrawn.

*Hopper section* – the converging part of a storage vessel that has sloped walls and a variable cross section.

*Mass flow* – flow pattern inside a bin where all material is in motion when withdrawn.

*Pressure* – force per unit area applied to an object in a direction perpendicular to the surface; same as compressive stress.

*Process vessel* – a bin that has been modified to allow heating, cooling, drying, reacting, or other processes to take place. Frequently they are equipped with heat exchangers or distributors for gas injection.

*Stress* – force per unit area, a tensor quantity.

## **Flow Problems**

Many storage vessels are fabricated from architectural or fabrication viewpoints (*e.g.*, hopper walls sloped 30° from vertical for ease of fabrication or 45° to minimize headroom requirements and simplify design calculations). However, designing equipment without regard to the bulk material being handled often leads to flow problems. Common solids flow problems include:

*No flow.* If a stable dome, bridge, or arch forms over the outlet of a bin, the bulk solid will not flow when the feeder is started or gate is opened. If a stable rathole forms in a vessel in which flow only occurs in a narrow channel above the outlet, material will stop flowing when the flow channel empties. Obstructions to flow are illustrated in Figures 2 and 3.

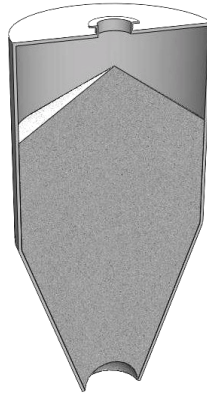


**Figure 2. Cohesive arch.**

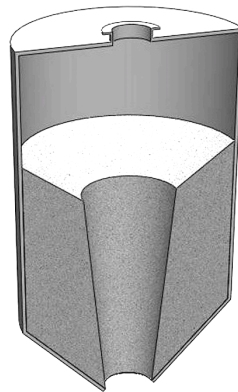


**Figure 3. Stable rathole.**

*Erratic flow.* Erratic flow occurs when both arching and ratholing occurs. If a rathole collapses due to external vibration, the bulk solid may arch as it impacts the outlet. After the arch fails due to vibration or operator intervention, the flow channel will empty leaving a rathole momentarily stopping flow until it eventually collapses, reforming a cohesive arch.

*Flooding.* If a stable rathole develops and fresh material is added or if a rathole collapses and falls into the channel, the material may become aerated or fluidized. Since most feeders are designed to handle solids and not fluids, the fluidized material may flood, that is, discharge uncontrollably in a fluidized state from the bin, and the feeder will not be able to control the rate of discharge.

*Limited discharge rate.* Because a fine powder dilates as it flows toward the outlet, vacuum will naturally develop inside the hopper above the outlet. As a consequence, air will flow counter to the solids, disrupting flow. Increasing the speed of the feeder will no longer increase the discharge rate of powder as the discharge rate has become limited.

*Caking.* Some materials will readily flow from a bin, portable container or bag if handled continuously or even after time at rest. Other materials, however, will exhibit flow problems if allowed to remain at rest for a period of time. Given enough time at rest, some bulk solids will gain additional cohesive strength, and obstructions to flow (*e.g.*, arches and ratholes) or hard lumps may become exceptionally difficult to eliminate.

*Segregation.* Some materials, when transferred into a bin or pile, will segregate, that is, particles of different size, shape, density, *etc.* will separate. Segregation can occur by a number of different mechanisms, depending on the physical characteristics of the particles and the method of handling.

### Flow Patterns

There are three primary flow patterns that can occur in a bin: *mass flow*, *funnel flow*, and *expanded flow*. Mass flow and funnel flow are illustrated in Figure 4.

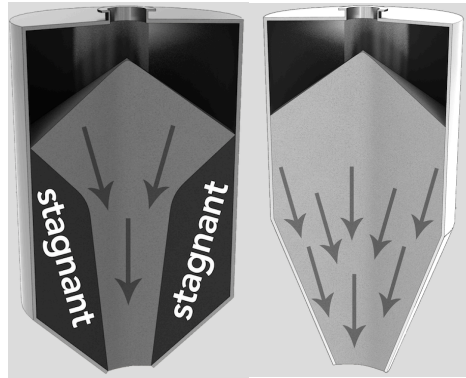


**Figure 4. Flow patterns – funnel flow (left) and mass flow (right).**

In *funnel flow*, an active flow channel forms above the outlet, with stagnant material remaining at the periphery. This occurs when the walls of the hopper section of the storage vessel are not steep enough or have low enough friction to allow flow along them. The size of the resultant flow channel is approximately the largest dimension of the outlet. It is equal to the diameter of a round outlet or the diagonal of a slotted outlet. In the case of conical funnel flow bins, the fraction of the vessel volume that is active can be dramatically small. If the bulk material is cohesive, a stable rathole will form thereby reducing the effective capacity of the bin to a small fraction of its intended capacity.

A funnel flow bin typically exhibits a first-in last-out flow sequence. Therefore, materials that readily cake or degrade over time should not be handled in funnel flow hoppers. Funnel flow can cause erratic flow and induce high loads (depending on vessel size) on the structure and downstream equipment due to collapsing ratholes and eccentric flow channels. If the bulk solid is cohesive, ratholes may become stable, and the vessel will not empty.

Funnel flow bins are best suited for bulk solids that are free flowing and do not degrade or gain strength over time. They should not be used if segregation is a concern. Funnel flow bins require less headroom and in general are less expensive to build than mass flow bins since they can have shallower walls.

In *mass flow*, the entire bed of solids is in motion when material is discharged from the outlet, including material along the walls. Mass flow bins typically have steep and/or low-friction walls. Provided that the outlet is large enough to prevent arching, all material will be discharged from the hopper, since ratholes cannot form.

Mass flow bins are characterized by a first-in, first-out flow sequence and therefore are suitable for handling materials that degrade with time or are prone to caking. The steep hopper walls provide a

more uniform flow than funnel flow bins, making mass flow hoppers suitable for process vessels. Discharge rates are predictable and steady, since the bulk density of the material at the outlet is nearly independent of the head of the material inside the vessel. Segregation by the dusting or sifting mechanism is minimized, as fine and coarse particles separated during filling are remixed at the outlet during discharge. A disadvantage of a mass flow bin is that it requires more headroom due to its steep hopper section. This is especially the case for conical mass flow bins.

*Expanded flow* is characterized by mass flow in the lowermost section of a bin and funnel flow in the upper section. An expanded flow bin is illustrated in Figure 5.

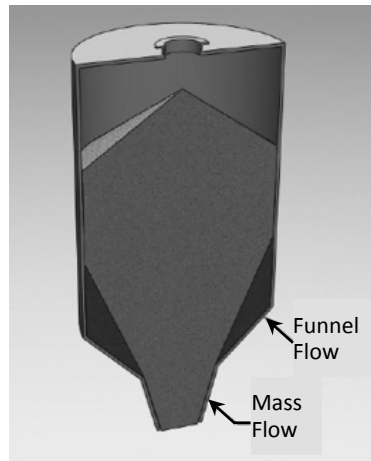


**Figure 5. Expanded flow pattern.**

The outlet of the funnel flow section must be large enough to prevent a stable rathole from developing. Because the bottom section is designed for mass flow, discharge rates are uniform and predictable. Expanded flow hoppers are frequently used when large bin diameters are required.

## ANALYSIS OF STRESS

Bulk solids are anisotropic; their stresses vary with direction. Although a bulk solid consists of individual particles, it is convenient to describe a bulk material as a continuum. A bulk solid element is sketched in Figure 6. The stresses acting normal (*i.e.*, perpendicular to) the element in the  $x$  and  $y$  directions are denoted  $\sigma_x$  and  $\sigma_y$ , respectively. The shear stresses acting in the  $x$  and  $y$  directions are denoted  $\tau_{yx}$  and  $\tau_{xy}$ , respectively.

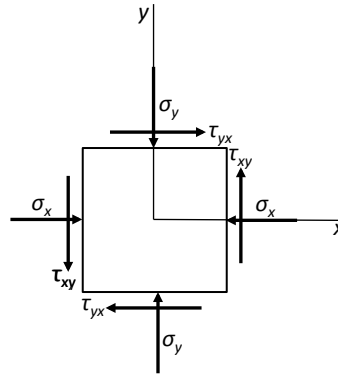


**Figure 6. Stress on an element of bulk solid.**

Given a state of stress, the magnitude of the normal and shear stresses acting on the bulk material will depend on the coordinate system used to describe the direction of these stresses. A new set of axes, denoted by  $x'$  and  $y'$ , rotated an angle  $\theta$  from the original axes, is shown in Figure 7.

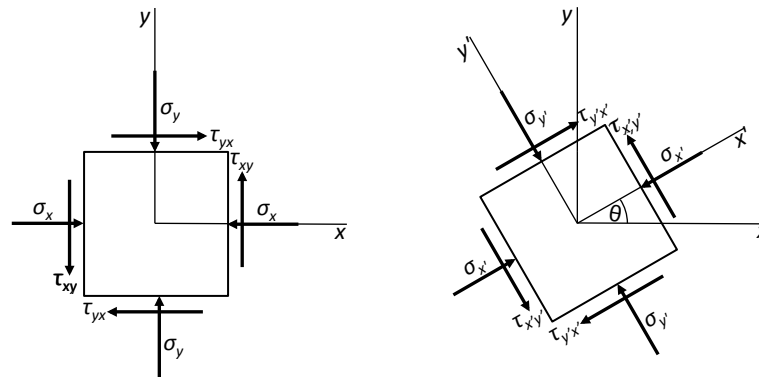


**Figure 7. Stresses on a rotated element.**

The stresses in terms of the new coordinate system are given by the following stress transformation equations:

$$\sigma_{x'} = \frac{\sigma_x + \sigma_y}{2} + \frac{\sigma_x - \sigma_y}{2} \cos 2\theta + \tau_{xy} \sin 2\theta \quad (1)$$

$$\sigma_{y'} = \frac{\sigma_x + \sigma_y}{2} - \frac{\sigma_x - \sigma_y}{2} \cos 2\theta - \tau_{xy} \sin 2\theta \quad (2)$$

$$\tau_{x'y'} = -\frac{\sigma_x - \sigma_y}{2} \sin 2\theta + \tau_{xy} \cos 2\theta \quad (3)$$

When analyzing solids, the maximum and minimum stresses frequently must be identified. These stresses are called principal stresses and can be readily found using a Mohr's circle, which can be derived from the stress transformation equations. A Mohr's circle is illustrated in Figure 8 and is described by:

$$(\sigma_x - \sigma_{avg})^2 + \tau_{xy}^2 = R^2 \quad (4)$$

where

$$\sigma_{avg} = \frac{\sigma_x + \sigma_y}{2} \quad (5)$$

and

$$R^2 = \left( \frac{\sigma_x - \sigma_y}{2} \right)^2 + \tau_{xy}^2 \quad (6)$$

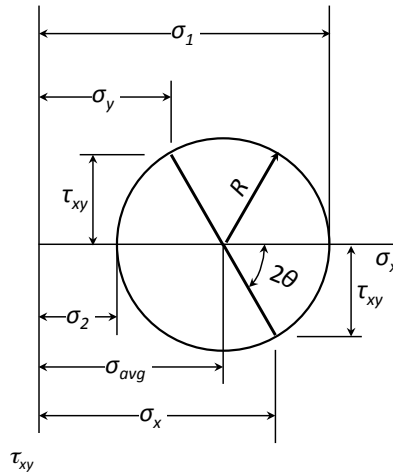


**Figure 8. Stress formation using a Mohr's circle.**

Note that the Mohr's circle is centered at  $\sigma_{avg}$  and the two points  $(\sigma_x, \tau_{xy})$  and  $(\sigma_y, -\tau_{xy})$  lie on opposite sides of the circle. To determine the stresses with respect to the rotated or transformed axes, the line connecting the two points  $\sigma_x, \tau_{xy})$  and  $(\sigma_y, -\tau_{xy})$  is rotated  $2\theta$ .

The maximum and minimum values of the normal stresses, *i.e.*, the major and minor principal stresses, respectively, can be determined from the two intersection points of the Mohr's circle and the horizontal axis. The major principal stress  $\sigma_1$  and minor principal stress  $\sigma_2$  can therefore be calculated from

$$\sigma_1 = \sigma_{avg} + R \quad (7)$$

$$\sigma_2 = \sigma_{avg} - R \quad (8)$$

## SOLIDS-INDUCED LOADS

The geometry of the bin and the solids flow properties, which determines the solids flow pattern, prescribe the pressure profiles that develop within the bulk solids during initial fill and discharge. Solids-induced load analyses are used to determine vessel wall thicknesses and reinforcements for structural integrity and the load on feeders, which is needed to determine power requirements.

A typical bin consists of a vertical (cylinder) section followed by a converging (hopper) section. Solids stresses are illustrated in Figure 9.

In the cylindrical section, the vertical and wall stresses increase with depth, tending asymptotically towards a maximum. The wall stresses are smaller than the vertical stresses by a factor equal to  $k$ . At the centerline of the bin the major principal stresses act vertically downward, and the minor principal stresses act horizontally.

When a previously empty bin is initially filled with a bulk solid, the major principal stresses in the converging section act vertically downward at the centerline. This stress state after initial fill is called the active stress state. A discontinuity exists in the wall stress profile. Both the wall stresses and vertical stresses decrease toward the hopper outlet.

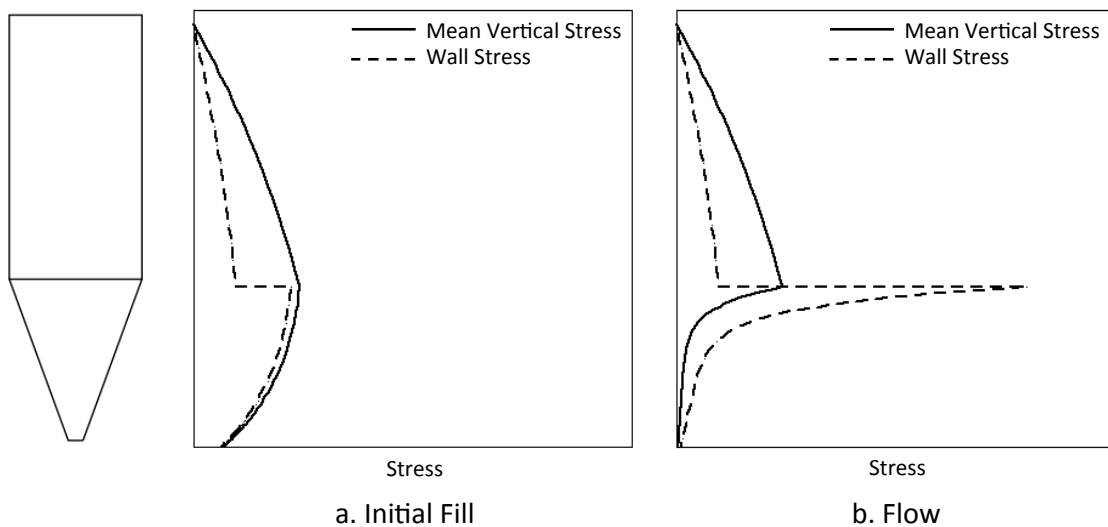


**Figure 9. Representative stress profiles in a mass flow bin; wall stress acts normal to the cylinder or hopper walls.**

When material is discharged from the bin, the stress conditions in the hopper section change if mass flow develops. In order to flow, the bulk solid is compressed laterally and expands vertically. As a result, the major principal stresses act horizontally at the centerline. This state of stress is called the passive state. A peak stress, called the switch, occurs at the hopper-cylinder interface.



## Cylinder stresses

The stresses on the solids in the straight-walled section of a bin were originally calculated by Janssen [*Z. Ver. Dt. Ing.*, 39, 1045 (1895)]. An equilibrium force balance on a volume element of bulk solids yields the following differential equation:

$$\frac{d\sigma_v}{dz} + \frac{k \tan \phi'}{R_H} \sigma_v = \rho_b g \quad (9)$$

where  $\sigma_v$  is the vertical stress,  $z$  is the depth of the solids bed,  $R_H$  is the hydraulic radius,  $k$  is the Janssen coefficient, which is equal to the ratio of the stress acting perpendicular to the walls to the vertical stress,  $\rho_b$  is the bulk density,  $g$  is acceleration due to gravity, and  $\phi'$  is the wall friction angle, which is equal to the inverse tangent of the wall friction coefficient. If a constant bulk density is selected, Equation 9 can be integrated to give the Janssen equation:

$$\sigma_v = \frac{\rho_b g R_H}{k \tan \phi'} \left[ 1 - \exp\left(\frac{-k \tan \phi'}{R_H} z\right) \right] \quad (10)$$

The horizontal stress  $\sigma_h$  is given by:

$$\sigma_h = \frac{\rho_b g R_H}{\tan \phi'} \left[ 1 - \exp\left(\frac{-k \tan \phi'}{R_H} z\right) \right] \quad (11)$$

The value of  $k$  is typically in the range of 0.3 to 0.6. Note that unlike liquids, the maximum solids stress is proportional to the hydraulic radius of the cylinder and is independent of its height.

## Hopper section

Walker [*Chem. Eng. Sci.* 21, 11, 975 (1966)] and Walters [*Chem. Eng. Sci.*, 28, 1, 13 (1973)] analyzed the stresses in the hopper section by performing an equilibrium force balance on an elemental volume with converging sides. A differential equation results, which is generalized by Jenike, [Loeffler, F.J., and C.R. Proctor, eds., Unit and Bulk Materials Handling, Effect of Solids Flow Properties and Hopper Configuration on Silo Loads., ASME, 1980, pp 97-106] as:

$$\frac{d\sigma_v}{dz} - n \frac{\sigma_v}{z} = -g \rho_b \quad (12)$$

$$n = (m+1) \left[ k \left( 1 + \frac{\tan \phi'}{\tan \theta} \right) - 1 \right] \quad (13)$$

where  $\theta$  is the hopper angle (from vertical) and  $m$  is equal to 1 for a conical hopper and equal to 0 for a straight-walled hopper having a slotted outlet.

Integration yields the following [British Standard BS EN 1991-4:2006]:

$$\sigma_v = \frac{\rho_b g h}{n-1} \left[ \frac{x}{h} - \left( \frac{x}{h} \right)^n \right] + \sigma_{vht} \left( \frac{x}{h} \right)^n \quad (14)$$

where  $x$  is the vertical coordinate upwards from the hopper apex,  $h$  is the vertical height between the hopper apex and the cylinder-hopper transition, and  $\sigma_{vht}$  is the mean vertical stress on the solid at the transition after filling (as determined from Equation 10).

The wall stress  $\sigma_w$  is calculated from:

$$\sigma_w = k\sigma_v \quad (15)$$

The frictional traction  $\tau_w$  is determined from:

$$\tau_w = k\sigma_w \quad (16)$$

The value of the stress ratio  $k$  depends on the flow properties of the bulk material handled and the slope of the hopper walls. Methods described by Enstad [*Chem. Eng. Sci.*, 40, 10, 1273 (1975)] can be used to calculate the stress ratio.

### **Funnel flow hoppers**

In funnel flow hoppers, the wall friction is not fully mobilized. An effective wall friction angle is therefore determined per EN 1991-4:2006.

### **Eccentric loads**

Although more common with funnel flow, eccentric discharge, in which the flow channel formation is not concentric with the vertical section of the bin, can occur in mass flow as well. Eccentric discharge can occur when a single outlet is not centered or when multiple outlets do not discharge at the same rate. Eccentric flow can also occur if gates or valves are partially opened or if feeder interfaces are not properly designed.

Asymmetric pressures develop on the walls when eccentric discharge takes place. A procedure for calculating discharge loads during eccentric flow is described in BS EN 1991-4:2006.

Note that the formulas for calculating normal pressures and shear tractions hereinabove do not include inherent factors-of-safety. A prudent designer must recognize that factors-of-safety are always necessary to account for unexpected loading conditions or deficiencies in the ability of the structure to withstand these loads. The designer is ultimately responsible for choosing the appropriate safety factor based on risks associated with structural failure and compliance with applicable design codes. Qualified engineers should review results of load analyses.

## BULK SOLIDS FLOW PROPERTIES TESTING

Designing systems for bulk solids can be challenging since they have a wide range of characteristics, e.g., cohesive or free-flowing; fine or coarse; fluffy or dense; adhesive to surfaces or surface repellent; easily aerated or nearly impermeable; and highly compressible or nearly incompressible. Defining a particle size distribution, density, or permeability is relatively straightforward. The best metric for cohesion or adhesion is not as obvious. Various characteristics or a combination of them are needed to define a bulk material's ease of flow or "flowability". However, even this is not enough, since "flowability" also depends on the design of the vessel from which the material is flowing – or is attempting to do so.

Several methods exist for measuring the *relative* flowability of bulk materials. The simplest is to determine the bulk solid's angle of repose by pouring it onto a horizontal surface and measuring the surcharge angle of the pile that is formed. A material that forms a steeper pile is believed to be less flowable than one that is shallow. However, as stated by Jenike [Storage and Flow of Solids, Bulletin 123, University of Utah, 1964 (revised, 1980)],

*"The angle of repose is not a measure of the flowability of solids. In fact, it is useful only in the determination of the contour of a pile, and its popularity among engineers and investigators is due not to its usefulness but to the ease with which it is measured."*

A compressibility test is another relative measure of flowability. A sample of bulk solid is vibrated or compacted ("packed") inside a rigid container, and its change in bulk density is measured. Two common methods to analyze the results are the Hausner ratio and Carr compressibility. The former is the ratio of the "tapped" density to the aerated or loose bulk density. The latter is determined by dividing the difference between the packed and freely settled bulk density by the packed bulk density. A low Hausner ratio or Carr compressibility supposedly indicates that the material is easy to handle. However, these indices are of limited use, since at best, they can be only loosely correlated to the flow behavior of similar bulk solids. In addition, these methods are deficient as the stress applied to the sample of bulk solid is unknown, the tests do not replicate the degree of consolidation that takes place when a material is stored in a vessel, and the gain in the material's strength during rest cannot be determined.

Solids rheometers of various designs are sometimes used to quantify the relative flowability of bulk solids. The material is placed in a cell equipped with an impeller, and the torque or energy required to rotate the agitator is measured. In some instruments, the vertical force on the agitator can also be directly measured. Flowability is deemed to correlate with the torque or the power drawn by the agitator. Unfortunately, the stresses acting in the shear zone during testing are unknown, and therefore the results cannot be applied to actual process conditions. In addition, both fluidization and agglomeration can occur inside the test cell, confounding the results. High torque or energy consumption may be the result of high friction between the bulk material and the walls of the cell, rather than an indication of the material's cohesive strength. Test methods based on stirred vessels therefore have questionable utility [Schulze, *Powders and Bulk Solids: Behavior, Characterization, Storage and Flow*, Springer, 2007].

There are five fundamental bulk solid flow properties that provide useful and reliable information from which one can design a bin for reliable flow: cohesive strength, internal friction, bulk density, wall friction, and permeability.

In contrast to fluids, materials having the same composition frequently have dramatically different fundamental flow properties. This is because flow properties are often dependent on the material's particle size, shape, and particle size distribution. In addition, temperature, moisture content (or the relative humidity of the material's interstitial air), purity, surface energy, and morphology all can influence the flow behavior of a bulk solid. The flow properties of many materials change when they are stored at rest.

There is no substitute for measuring the flow properties of the actual materials that are to be handled, and testing should be performed over a range of temperatures, moisture contents, relative humidity levels, time at rest, and stress levels at which the bulk solid will be stored and handled. Using flow property data from the literature or assuming that the properties are the same as those of other materials whose properties are known is extremely risky. For example, "coal" in an extremely non-homogeneous material; yet some textbooks and design codes provide values (a limited range or sometimes a single value) of important design parameters such as bulk density and wall friction. Such tabular data are, at a minimum, misleading and potentially worse than having no data at all.

### **Cohesive strength and internal friction**

A bulk solid gains cohesive strength when consolidated in a bin. The size of the outlet of the vessel that will prevent arching or the formation of a stable rathole depends greatly on the bulk material's cohesive strength.

Figure 10 is a schematic of a uniaxial compressive strength tester. In a uniaxial test, a sample is placed in a cell with nearly frictionless walls and is then consolidated by applying a stress equal to  $\sigma_1$ . Next, the load and cell are removed. The compacted specimen is then loaded with increasing compressive stress until it breaks apart, *i.e.*, fails. The failure stress is called the material's cohesive strength or the unconfined yield strength  $f_c$ .

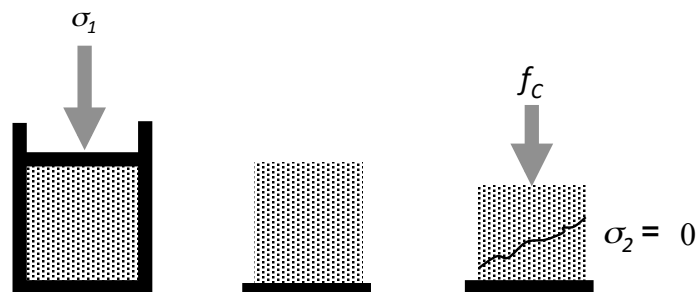


**Figure 10. Uniaxial compressive strength test.**

Uniaxial compressive strength test results are often highly variable. Improvements have been made to uniaxial strength testers to reduce their variability; however, uniaxial compression tests usually do not provide a bulk material's true unconfined yield strength, and therefore the cohesive strength of a

bulk solid is best measured by direct shear cell testing. Translational (Jenike), annular (ring), and rotational testers are frequently used. They are described in ASTM standards D-1628 (translational), D-6773 (annular), and D-6682, and D7891 (rotational). Schematics of the testers are given in Figure 11.

The direct translational shear tester was originally developed by Andrew Jenike [Storage and Flow of Solids, Bulletin 123, University of Utah, 1964 (revised, 1980)]. This tester is particularly robust in that its cell can be placed in extreme environments allowing a material's cohesive strength to be measured over a full spectrum of process conditions. Its disadvantage is that significant operator training and experience are usually required to be able to obtain reproducible results.

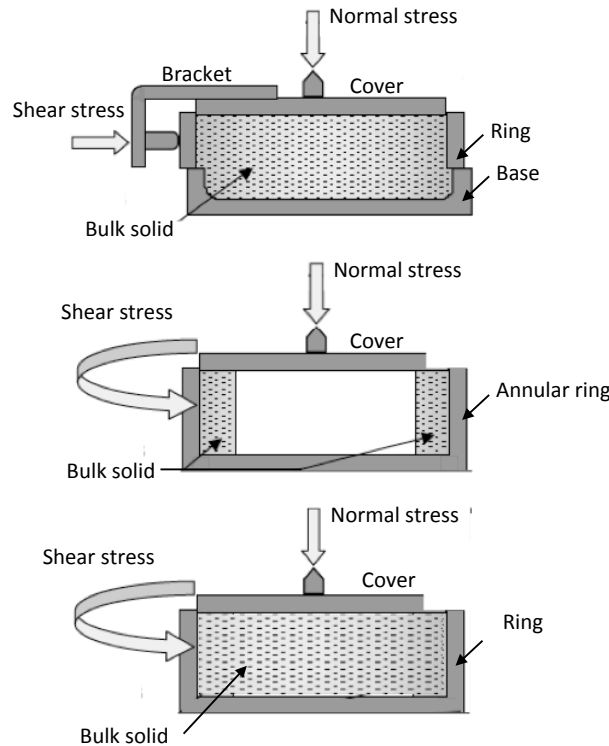


**Figure 11. Shear cell testers – Jenike direct (top), annular (middle) and rotational (bottom).**

Modern annular and rotational shear testers are computer controlled and are thus more straightforward to operate and less prone to operator variability than manually controlled shear testers.

In a rotational shear cell, shear deformation of the specimen varies with radius in the cell: at the perimeter it is at its maximum, while at the center it is zero. This can result in data that differ from results obtained using a Jenike (translational) or annular shear cell. Rotational and annular shear cells permit infinite travel, so they are better suited than a Jenike shear cell for testing bulk solids that require large shear strain to reach steady state. The Jenike shear cell tester can be relatively easily modified to operate at high or low temperatures, whereas this is more difficult if not impossible with the other two types of testers.

Cohesive strength is measured by shear cell testing as described in ASTM D-1628, D-6682, D-6773 or D7891. A sample of bulk material is placed in a cell and then pre-sheared, *i.e.*, consolidated by exerting a normal stress and then shearing it until the measured shear stress is steady (as illustrated by the point  $(\sigma_{ss}, \tau_{ss})$  shown in Figure 12). Next, the shear step is conducted, in which the vertical compacting load is replaced with a smaller load, and the sample is again sheared until it fails. These pre-shear and shear steps are repeated at the same consolidation level for a number of reduced normal stresses, and the yield locus is then determined by plotting the failure shear stress against normal stress (see Figure 12).

Ideally, all measurements of the pre-shear shear stress  $\tau_{ss}$  should be identical. However, because of unavoidable variability during testing, there is inevitably scatter in the  $\tau_{ss}$  values. Prorating is used to account for the variability of the data [Jenike, 1964].

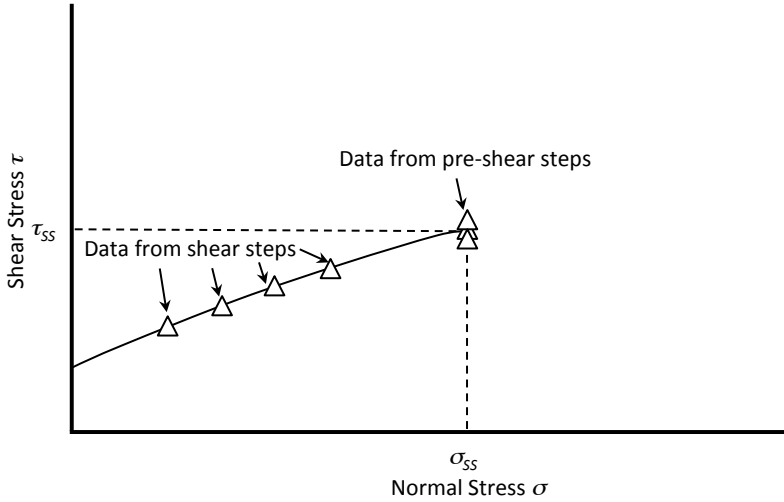


**Figure 12. Yield locus.**

To determine the major consolidation stress  $\sigma_l$  and the unconfined yield shear strength  $f_c$  from the yield locus, a line is drawn through the shear step data. A Mohr’s semicircle is then drawn through the steady-state result  $(\sigma_{ss}, \tau_{ss})$  tangent to the yield locus line (see Figure 13).

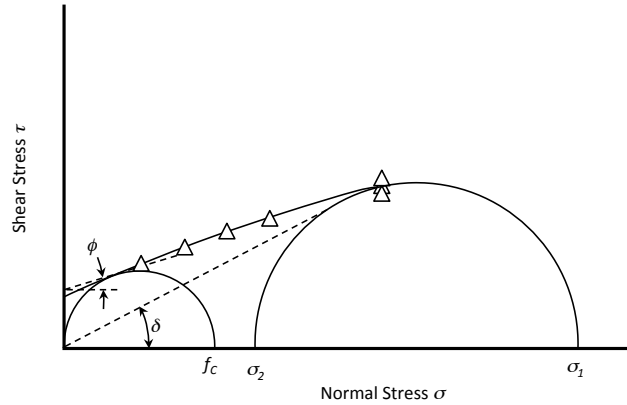


**Figure 13. Linear yield locus.**

The larger point of intersection of the semicircle with the horizontal axis gives the value of the major consolidating stress  $\sigma_1$ . The unconfined yield strength  $f_c$  is determined by drawing a Mohr's semicircle tangent to the yield locus and passing through the origin. The point of intersection of this circle and the horizontal axis is the unconfined yield strength, which can be considered the cohesive strength of the bulk solid. Note that all points on the yield locus should lie to the right of the point of tangency to the smaller Mohr's circle.

Also determined are the effective angle of friction and kinematic angle of internal friction ( $\delta$  and  $\phi$ , respectively). The effective angle of friction is found by constructing a line through the origin and tangent to the larger Mohr's semicircle. The kinematic angle of internal friction is the angle formed between a line that is horizontal and one drawn tangent to the smaller Mohr's circle at its intersection with the yield locus (see Figure 13).

The yield locus generally is slightly concave downward, but with many particulate solids a straight line is a sufficient approximation. If the yield locus is approximated as a straight line for all particulate solids, then subsequent calculations are much simpler, but, in some cases, somewhat conservative results may be obtained, that is, a higher  $f_c$  value will be determined than when using a fitted curve. The shear data that make up the yield locus (*i.e.*, all data points *sans* the steady-state or pre-shear data) are regressed to give the following linear relation:

$$\tau = c + \sigma \tan \phi \quad (17)$$

where  $\tau$  is the shearing stress and  $\sigma$  is the normal stress. Equation 17 is the Coulomb equation. The slope of the line is equal to the tangent of the kinematic angle of internal friction  $\phi$ , and the intercept is equal to  $c$ , which is called the material's cohesion.

The unconfined yield strength and major consolidation stress are then calculated from:

$$f_c = \frac{2c(1 + \sin \phi)}{\cos \phi} \quad (18)$$

and

$$\sigma_1 = \left( \frac{A - \sqrt{A^2 \sin^2 \phi - \tau_{SS}^2 \cos^2 \phi}}{\cos^2 \phi} \right) (1 + \sin \phi) - \frac{c}{\tan \phi} \quad (19)$$

respectively, where

$$A = \sigma_{SS} + \frac{c}{\tan \phi} \quad (20)$$

The minor consolidation stress  $\sigma_2$  can be calculated from

$$\sigma_2 = \sigma_{SS} - \frac{\tau_{SS}^2}{(\sigma_1 - \sigma_{SS})} \quad (21)$$

Finally, the effective angle of friction  $\delta$  is calculated from:

$$\delta = \sin^{-1} \left( \frac{\sigma_1 - \sigma_2}{\sigma_1 + \sigma_2} \right) \quad (22)$$

A straight line through the origin of the  $\sigma$ - $\tau$  diagram, tangent to the larger Mohr's circle, is the effective yield locus (EYL). The larger Mohr's circle can be constructed by drawing a circle having a radius  $R$  that passes through  $\sigma_1$  on the horizontal axis. The radius  $R$  is given by

$$R = \frac{\sigma_1 - \sigma_2}{2} \quad (23)$$

Construction of the effective yield locus is illustrated in Figure 14.

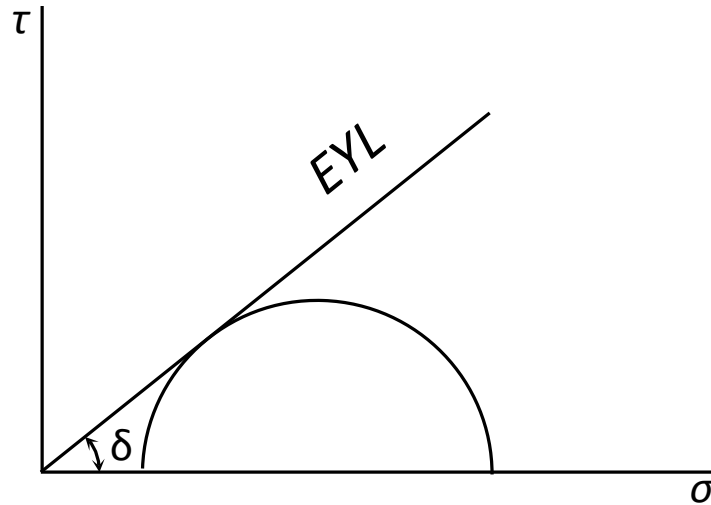


**Figure 14. Construction of the effective yield locus.**

Plotting values of  $f_c$  against the major consolidation stress  $\sigma_1$  gives the Flow Function of the bulk solid. The Flow Function describes the relationship between a bulk material's unconfined yield



strength and its state of consolidation. Construction of the Flow Function from a number of yield locus measurements is illustrated in Figure 15.

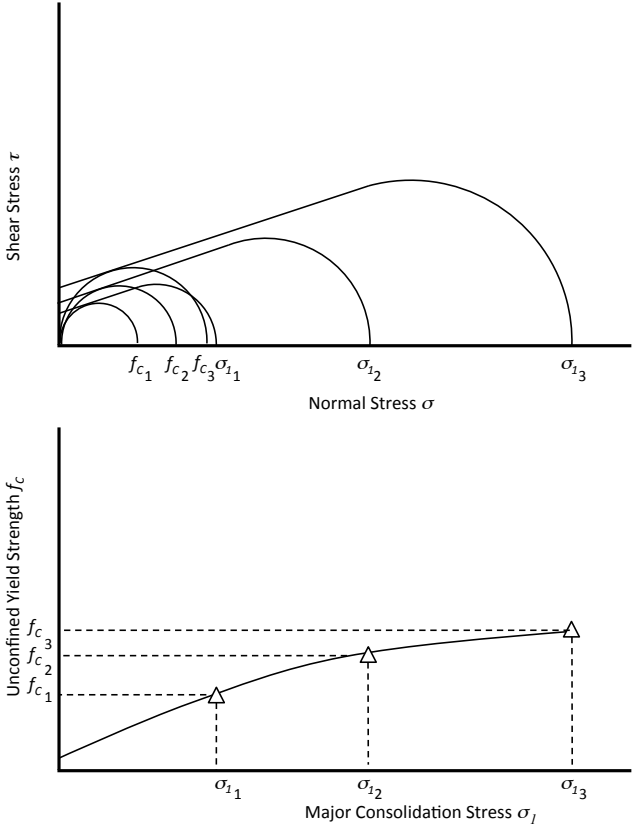


**Figure 15. Construction of Flow Function from yield loci.**

Some bulk materials gain cohesive strength if stored at rest. Unless a bin is expected to be operated continuously, the time unconfined yield strength of the bulk material should be measured. To conduct a time test, a sample of bulk material is placed inside a cell and pre-sheared using a normal stress  $\sigma_{ss}$  used during instantaneous testing. After pre-shear, the sample is then kept consolidated at that state of stress, typically by applying a vertically-acting load equal to the major consolidation stress  $\sigma_I$  associated with the corresponding instantaneous test. After the time of interest has passed (e.g., 2-3 days if the bulk material is to be stored at rest over a weekend), the vertical compacting load is replaced with a smaller load, and the shear step is conducted, in which the shearing force again is applied until the sample fails.

The pre-shear, time consolidation, and shear steps are repeated at the same normal stress  $\sigma_{ss}$  for a number of normal stresses, and the time yield locus (TYL) is then determined by plotting the failure shear stress against normal stress. An example of a time yield locus is given in Figure 16.

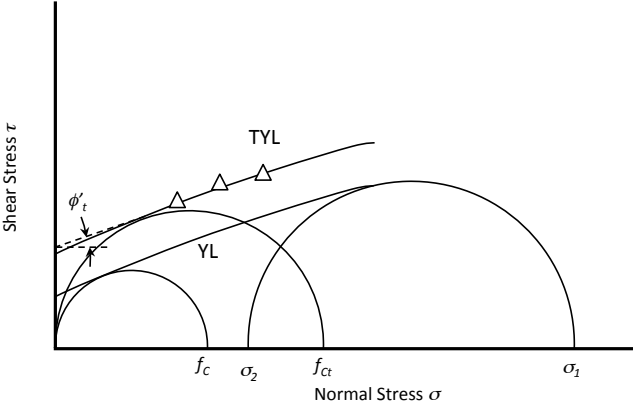


**Figure 16. Construction of the time yield locus.**

To calculate the time unconfined yield strength, a Mohr's circle is drawn through the origin and tangent to the time yield locus. The point of intersection with the horizontal axis is the material's time unconfined yield strength  $f_{ct}$ . This value, along with the value of the major consolidation stress for instantaneous flow  $\sigma_1$ , becomes one point on the *time* Flow Function.

The time angle of internal friction  $\phi_t$  is the angle formed between a horizontal line and a line drawn tangent to the smaller Mohr's circle at its intersection with the time yield locus (see Figure 16).

By measuring time yield loci using other normal stress levels and corresponding major consolidation stresses, the time Flow Function can be determined by plotting the time unconfined yield strength  $f_{ct}$  against major consolidation stress  $\sigma_1$ . If a bulk material gains strength when stored at rest in a bin over time, its time Flow Function will lie above its instantaneous Flow Function, as illustrated in Figure 17.

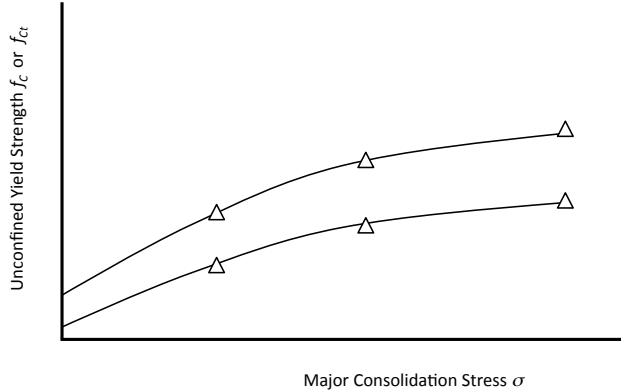


**Figure 17. Instantaneous and time Flow Functions.**

Because of the obvious time-consuming nature of a time consolidation test, extra test cells should be used so that the sample after pre-shear can be kept consolidated outside the shear tester.

## Bulk density

A method to measure the bulk density of a material as a function of compressive stress (*i.e.*, pressure) is given in ASTM D6683. A sample is placed in a cylinder of known volume and its mass is recorded. A lid with a known weight is placed on the specimen and the displacement is noted, allowing an updated volume to be calculated. The consolidation pressure is equal to the weight placed on the sample divided by the cross-sectional area of the cylinder. The bulk density is equal to the mass of sample divided by the volume. Increasing loads are placed on the lid, and the displacement is recorded for each load. From the data, the bulk density as a function of consolidation pressure is determined. A typical bulk density curve is shown in Figure 18.

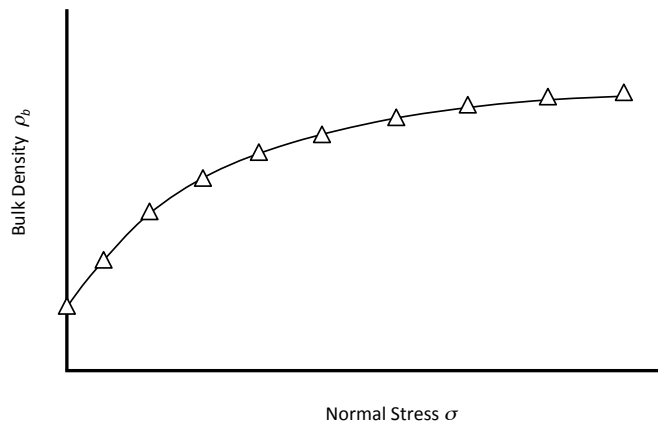


**Figure 18. Typical bulk density – consolidation stress relationship.**

The relationship between bulk density and consolidation stress is nonlinear. The bulk density increases with increasing consolidation pressure, varying rapidly at low stress and less so at high stress. Data can be fit to a number of equations that describe the relationship between bulk density and consolidation pressure. Jenike and Johanson [*Powder Techn.* 5, 133 (1971/72)] assumed a power-law relationship:

$$\rho_b = \rho_{b0} \left( \frac{\sigma}{\sigma_0} \right)^\beta \quad (24)$$

where  $\sigma$  is the consolidation pressure,  $\sigma_0$  is an arbitrarily chosen reference consolidation level,  $\rho_{b0}$  is the bulk density at that consolidation, and  $\beta$  is called the compressibility. A limitation of the model is that at zero stress, Equation 24 gives a bulk density equal to zero. Hence, at a low consolidation pressure, the bulk density is limited to no less than  $\rho_{bmin}$ , the loose-fill bulk density.

Ideally, a model that describes the bulk density – consolidation pressure relationship should give a bulk density of  $\rho_{min}$  at zero consolidation. Some relationships that meet this criterion are [Gu *et al.*, *Powder Techn.*, 72, 39 (1992)]:

$$\rho_b = \rho_{bmin} (1 + \alpha\sigma)^\beta \quad (25)$$

$$\rho_b = \rho_{b\min} + \alpha\sigma^\beta \quad (26)$$

$$\begin{aligned} \rho_b &= \rho_{b\min}, & \sigma &= 0 \\ \rho_b &= \rho_{b\min} + \frac{(\rho_{b0} - \rho_{b\min})\sigma}{\rho_{b0}}, & 0 < \sigma < \sigma_0 \\ \rho_b &= \alpha\sigma^\beta, & \sigma &\geq \sigma_0 \end{aligned} \quad (27)$$

$$\rho_b = \rho_{b\max} - (\rho_{b\max} - \rho_{b\min})\exp(-\alpha\sigma) \quad (28)$$

$$\rho_b = \rho_{b\min}\rho_{b\max} \frac{1 + \alpha\sigma}{\rho_{b\max} + \rho_{b\min}\alpha\sigma} \quad (29)$$

where  $\alpha$  and  $\beta$  are empirical constants and  $\rho_{b\max}$  is the material's maximum bulk density.

### Wall friction

The flow pattern inside a bin depends on the friction between the bulk solid and the wall material. Therefore, measuring wall friction is one of the necessary steps to design reliable bulk solids storage vessels.

To measure the friction between a bulk solid and a wall material, the method described in ASTM D-6128 is usually followed. The test is conducted using a direct translation shear tester. A sample of bulk solid is placed inside a retaining ring on a flat coupon of wall material (see Figure 19), and a load is then applied normal (*i.e.*, perpendicular) to the bulk solid. The ring and bulk solid in the ring are forced to slide along the stationary wall material, and the resulting steady shear force is measured as a function of the applied normal load. The normal load is then reduced, and the test is continued until a new steady shear load is measured. The test is repeated for various normal loads.

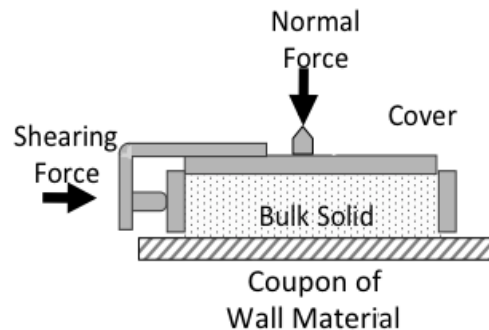


**Figure 19. Wall friction test equipment.**

In most industrial applications, the wall surface upon which a bulk solid is sliding is below the bulk solid. Due to the segregating nature of some bulk solids, differences in wall friction angles may be

observed between testers where the wall friction coupon is placed above the test cell and those, such as the Jenike shear cell, where the wall friction coupon is located below.

The direction of grain orientation of a wall surface usually has a dramatic effect on wall friction angle. This effect can be captured in the Jenike shear cell but not in rotational or annular shear cells.

After a number of steady shear load values have been recorded, the *instantaneous wall yield locus* (WYL) is constructed by plotting shear stress against normal stress. The angle of wall friction  $\phi'$  is the angle that is formed when a line is drawn from the origin to a point on the wall yield locus. A typical wall yield locus is shown in Figure 20.

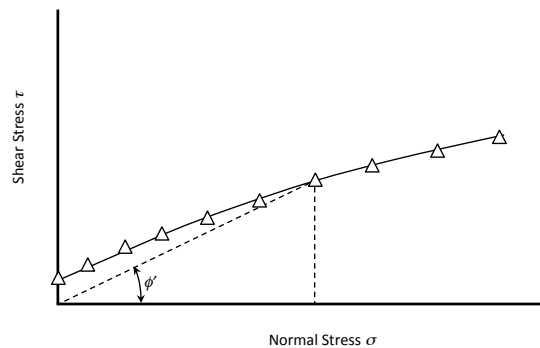


**Figure 20. Wall yield locus.**

The wall yield locus is typically concave downward. In addition, the wall yield locus does not necessarily intersect the origin, as many bulk materials adhere to a wall surface in the absence of a normal stress. As a consequence,  $\phi'$  is usually higher at lower applied stresses. This is important in the design of hoppers, since for mass flow, the stresses at the hopper outlet are low and the angle of wall friction is therefore usually higher near the outlet. Only when the yield locus is a straight line that passes through the origin is  $\phi'$  constant.

To measure the static friction between a wall surface and a bulk solid after storage at rest, wall friction time tests are performed. A sample is sheared under a normal load until a steady shear load is observed. The normal load is then reduced by 10-20 percent, and shearing is continued until steady state is again reached. This step is analogous to the procedure of obtaining a point on the instantaneous wall yield locus.

The shear is then reduced to zero and the sample is stored in the cell for the required period of time. After the storage time, the sample is again sheared, and the maximum shear load is reported.

The pair of normal stress and maximum shear stress values provide one point on the *time wall yield locus* (TWYL). Repeating the test at different normal loads completes the time wall yield locus. The time angle of wall friction is the angle obtained by drawing a line from the time wall yield locus to the origin (see Figure 21).

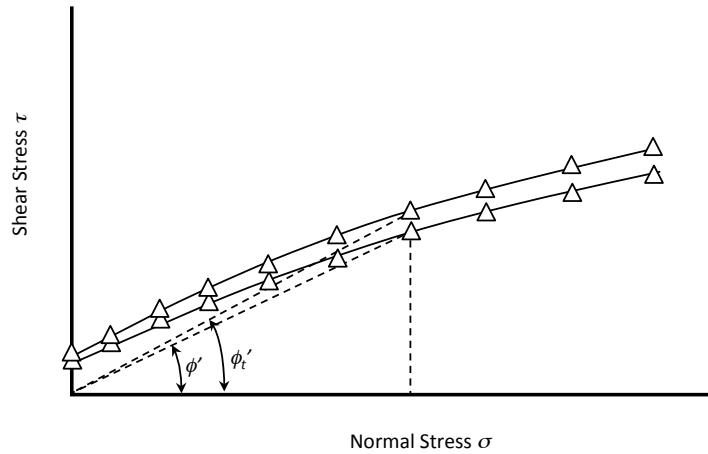


**Figure 21. Time wall yield locus.**

Changes in both the bulk solid's properties (due, for example, to changes in moisture content, temperature, *etc.*) and the wall surface (for example, due to surface finish, corrosion or abrasion) affect the wall friction angle. It is important that one not assume that a "smooth" surface, *i.e.*, one with a low  $Ra$  (average surface roughness) value, will necessarily be low in wall friction angle. Sometimes a surface with small asperities (which result in a larger  $Ra$  value) will be less frictional than a smoother surface.

### Permeability

The maximum achievable steady-stated discharge rate of a bulk material from a bin depends on its permeability. The pressure drop that arises when a gas passes through a bed of bulk solid is described by Darcy's law if the gas flow is laminar:

$$u_s = -\frac{K}{\rho_b g} \frac{dP}{dz} \quad (30)$$

where  $u_s$  is the superficial gas velocity,  $K$  is the bulk material's permeability, and  $dP/dz$  is the gas pressure gradient. Permeability is determined by measuring the pressure drop and gas flow rate using the apparatus shown in Figure 22.

The permeability of a bulk solid is highly dependent on its bulk density. The relationship between permeability and bulk density can be determined by filling the tester with compacted material. Often, the relationship between permeability and bulk density is described by a power-law relationship, *e.g.*,

$$K = K_0 \left( \frac{\rho_b}{\rho_{b0}} \right)^{-\alpha} \quad (31)$$

where  $\alpha$  is a constant,  $\rho_{b0}$  is a reference bulk density, and  $K_0$  is the permeability of the bulk solid measured at the reference bulk density.

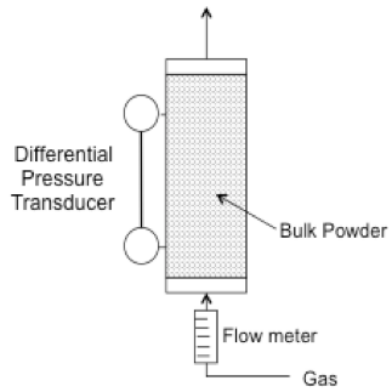


**Figure 22. Permeability tester.**

### **Abrasive wear**

Abrasive wear of equipment is a problem that should not be overlooked. It is important that solids contact surfaces be durable, thick enough to provide reasonable wear life, and, if necessary, replaceable to minimize maintenance.

Prediction of the wear rate can be accomplished in a two-step process. The first step is to determine the bulk solids velocity and compressive stress acting on the wear surface. The second step is to determine the rate of wear of the wear surface as a function of bulk solids stress using a suitable wear testing apparatus.

A suitable wear tester is one that continuously introduces a fresh supply of a bulk solid sample to a wear surface. The tester should continuously control and measure the relative velocity between the bulk solid and wear surface and the solids stress exerted on the wall material. Any changes in the wall friction angle can be determined by running a wall friction test before and after a certain number of cycles of the wear test.

A description of an abrasive wear tester is given in U.S. Patent No. 4,446,717. A sample of bulk solid is conveyed to a circular disc fabricated from the wear material, and a supporting frame applies and measures torque, thrust, and the number of revolutions. Tests are conducted over a range of expected solids stresses. Wear is measured as the weight loss of the sample disc after a certain number of revolutions of the disc.

It is convenient to define a wear ratio  $WR$  as the dimensionless ratio of unit thickness of material lost per unit distance travel of the bulk solid sliding relative to the wear surface.

The solids velocity at the hopper wall can be calculated using a method described by Johanson and Royal [*Bulk Solids Handling*, 2, 3, 517 (September 1992)] and is inversely proportional to the cross-sectional area of the hopper. The wear ratio is a function of the applied solids stress. Methods to calculate solids-induced loads were described previously. The wear rate is equal to the product of the wear ratio  $WR$  and the solids velocity at the wall. Because the solids velocity and stress vary inside the hopper, the degree of abrasive wear will vary with location.

## **BIN DESIGN**

When developing the *functional*<sup>1</sup> design of a new bin, there are a number of factors that determine what type of bin is required. These factors include the cohesiveness of the bulk solid, headroom or footprint constraints, segregation concerns, the likelihood of degradation over time (*e.g.*, caking, spoilage, spontaneous combustion), the location of the outlet relative to bin's centerline, and discharge rate requirements.

In general, for a given volume, mass flow hoppers, bins, and silos are taller than those designed for funnel flow. If there are headroom restrictions, designing a mass flow bin with the desired capacity may be challenging. Whenever this is the case, an engineer should confirm that the constraints are necessary or consider whether a funnel flow or expanded flow bin will suffice.

### **Mass Flow Hopper Angle**

Flow problems can often be prevented by ensuring that a mass flow pattern will develop in the vessel. The first step in achieving mass flow is to ensure that the converging walls are steep enough and have friction low enough to allow the bulk material to slide along them. This is accomplished by first testing the material to measure wall friction and then calculating the minimum hopper angle that will allow mass flow.

By assuming a radial stress field, Jenike [Gravity flow of Bulk Solids, Bulletin 108, University of Utah, 1961] was able to calculate stresses in the region of the hopper outlet as a function of the effective angle of friction  $\delta$ , hopper angle (from vertical)  $\theta'$ , and wall friction angle  $\phi'$ . Jenike determined that when the boundary conditions are not compatible with the radial stress equations, mass flow cannot occur in a hopper, and a funnel flow pattern results.

Design charts originally developed by Jenike [1961] provide allowable hopper angles for mass flow given values of wall friction angle and the effective angle of friction. These charts are summarized in Figures 23 and 24 for conical (or pyramidal) and planar hoppers (*e.g.*, wedge-shaped hoppers and transition hoppers), respectively. The outlet of a wedge-shaped or transition hopper must be at least two times as long as it is wide for Figure 24 to apply if it has vertical end walls and three times as long if its end walls are converging.

---

<sup>1</sup> A functional design includes hopper shape, hopper angles, outlet details, overall configuration, insert size and location (if one is needed), interior surface specifications for flow, liner material and installation considerations, details to avoid flow impediments, and considerations for proper gas flow where important.



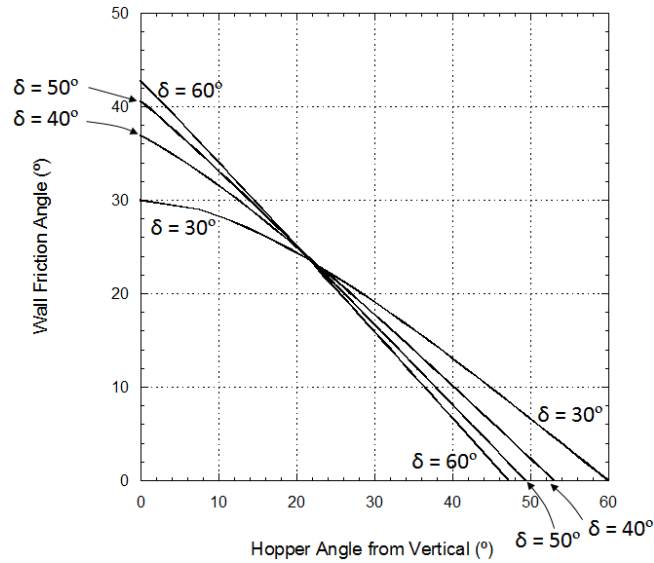


**Figure 23. Theoretical mass flow hopper angles for hoppers with round or square outlets.**  
*Note: a minimum safety factor of 3 to 5° should be used.*

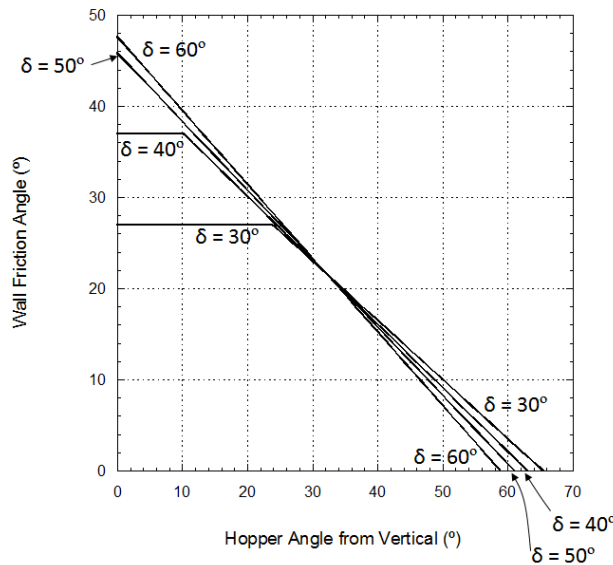


**Figure 24. Recommended mass flow hopper angles for wedge-shaped hoppers.**

Values of the allowable hopper angle for mass flow  $\theta'$  (measured from vertical) are on the abscissa, and values of the wall friction angle  $\phi'$  are on the ordinate. Any combination of  $\phi'$  and  $\theta'$  that falls within the mass flow region of the chart will provide mass flow.

An analytical description of the theoretical boundary between mass flow and funnel flow regions for conical hoppers is given in Enstadt [*Chem. Eng. Sci.*, 30, 1273 (1975)]; an explicit equation that gives recommended mass flow angles for hoppers with slotted outlets is provided by Arnold *et al.* [*Bulk Solids: Storage, Flow, and Handling*, TUNRA Publications, 1980].

Hoppers with round or square outlets should not be designed at the theoretical mass flow hopper angle value. Otherwise, a small change in the bulk material's flow properties may cause the flow pattern inside the hopper to change from mass flow to funnel flow, with its associated risk of flow problems. A 3 to 5° margin of safety with respect to the mass flow hopper angle given in Figure 23 is therefore recommended.

Sloping walls required for mass flow in wedge-shaped hoppers can be 10-12° less steep than those required to ensure mass flow in conical or pyramidal hoppers. In fact, hoppers with angles less steep than those given in Figure 24 may still allow flow along the walls. Planar flow hoppers are therefore highly suitable for materials that have high values of wall friction angle.

As illustrated in Figure 25, transition hoppers have both straight sides (side walls) and round sides (end walls). The appropriate chart or equation must be used in specifying the angles of the end walls (Figure 23) and side walls (Figure 24) when designing a transition hopper for mass flow.

Additional care must be taken when designing a pyramidal hopper for mass flow. The angles that are formed at the intersections of the sloping walls of pyramidal hoppers are significantly less steep than those of the hopper walls themselves. The valley angle from vertical  $\theta_v$  can be calculated from

$$\theta_v = \tan^{-1} \sqrt{\tan^2 \theta_{side} + \tan^2 \theta_{end}} \quad (32)$$

where  $\theta_{side}$  and  $\theta_{end}$  are the side and end wall angles from vertical, respectively. Side, end, and valley angles are defined in Figure 26.

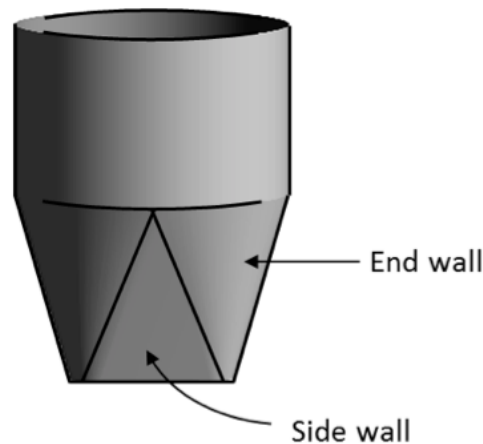


**Figure 25. Side and end walls of transition hopper.**

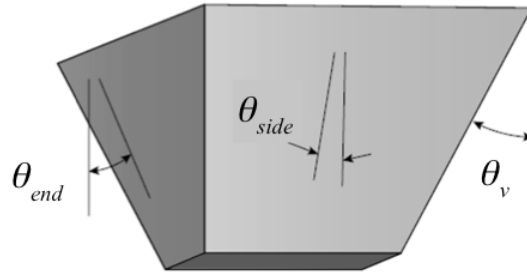


**Figure 26. Side, end, and valley angles of pyramidal hoppers.**

**Mass flow outlet dimensions to prevent arching**

The outlet of the hopper must be large enough to prevent stable obstructions to flow from developing. The required outlet size depends on the unconfined yield strength, the effective angle of friction, the bulk density of the bulk solid, and the flow pattern.

For an obstruction to flow to develop, the cohesive strength that the bulk solid gains as a result of its consolidation in the hopper must be able to support the weight of the obstruction. Jenike’s flow – no flow postulate is as follows [Jenike, 1964]:

*Gravity flow of a solid in a channel will take place provided the yield strength which the solid develops as a result of the action of the consolidating pressure is insufficient to support an obstruction to flow.*

In a mass flow bin, as an element of bulk material flows downward, it becomes consolidated under a major consolidation stress  $\sigma_l$  and develops an unconfined yield strength  $f_c$ . The consolidating stress follows the Janssen equation in the vertical section of the bin, sharply changes at the cylinder-hopper junction, and then decreases toward the outlet.

Jenike [1961] calculated the stress on the abutment of a cohesive arch over the outlet  $\bar{\sigma}$  as

$$\bar{\sigma} = \frac{\rho_b g B}{H(\theta')} \tag{33}$$

where  $B$  is the diameter of the outlet of a conical hopper or the width of the slotted outlet of a planar hopper, and the function  $H(\theta')$  given by Jenike [1961] is shown in Figure 27.  $H(\theta')$  can be calculated from [Arnold and McLean, *Powder Techn.*, 13, 255 (1976):

$$H(\theta') = \frac{130^\circ + \theta'}{65^\circ} \tag{34}$$

for round outlets, and

$$H(\theta') = \frac{200^\circ + \theta'}{200^\circ} \tag{35}$$

for slotted outlets.

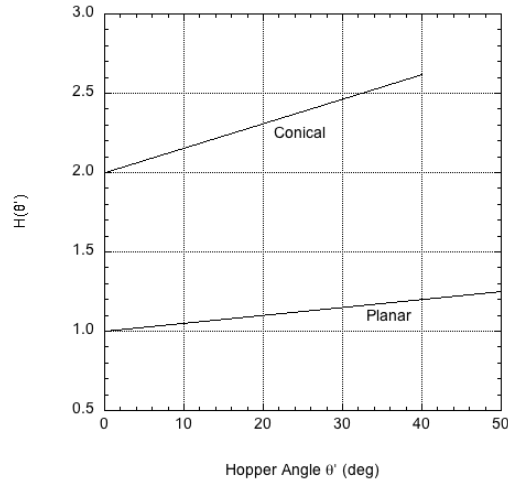


**Figure 27. Function  $H(\theta')$**

The stress and strength profiles inside a bin are shown in Figure 28. Note that there is a critical outlet size where the stress on the abutments of a cohesive arch is equal to the unconfined yield strength of the bulk solid. This outlet dimension represents the minimum outlet size that will prevent a stable cohesive arch from developing.

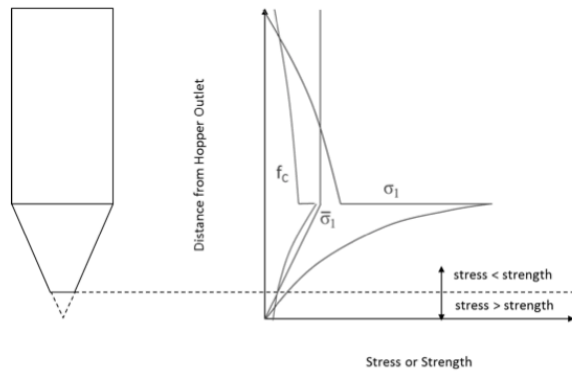


**Figure 28. Stress and strength profiles of mass flow hopper.**

Jenike postulated that near the hopper outlet the stress distribution of the bulk solid could be described by a radial stress field, *i.e.*, the stress distribution could be approximated by a straight line through the hopper vertex. The average stress was modeled as:

$$\sigma_{avg} = r\rho_b g s(\theta') \quad (36)$$

where  $r$  is the radial coordinate with the origin located at the vertex of the hopper,  $\sigma_{avg}$  is the average stress, and  $s(\theta')$  is called the stress function. Jenike [1961] developed solutions to the stress function and presented them in chart form.

The major consolidation stress is related to the average stress by

$$\sigma_1 = \sigma_{avg} (1 + \sin \delta) \quad (37)$$

At the hopper outlet,

$$\sigma_1 = \frac{B\rho_b g s(\theta')(1 + \sin \delta)}{2 \sin \theta'} \quad (38)$$

Jenike [1961] defined the ratio of the major consolidation stress to the arch support stress as the flow factor  $ff$ , that is,

$$ff = \frac{\sigma_1}{\sigma} \quad (39)$$

Hence, the flow factor is given by

$$ff = \frac{H(\theta')s(\theta')(1 + \sin \delta)}{2 \sin \theta'} \quad (40)$$

The flow factor is a function of the hopper angle  $\theta'$ , angle of wall friction  $\phi'$ , and the effective angle of friction  $\delta$ . The latter depends on the major consolidation stress  $\sigma_1$  at the hopper outlet. The angle of wall friction depends on the stress normal to the hopper wall  $\sigma'$ , which is *not* equal to  $\sigma_1$ .

Charts that provide flow factors for conical and planar flow hoppers based on Jenike's solutions to the stress function [Jenike, 1964] are given in Figures 29 through 36. Explicit expressions for the flow factor from an analytical form of the stress function were derived by Arnold and McLean [*Powder Techn.*, 13, 255 (1976); *Powder Techn.*, 72, 121 (1992)].

Superimposing the material's Flow Function and flow factor on the same graph allows the unconfined yield strength and arch stress to be compared. The flow factor is constructed by drawing a line having a slope equal to  $1/ff$  through the origin.

The relationship between the effective angle of friction  $\delta$  and the major consolidation stress  $\sigma_1$  is provided by the effective yield locus. In a converging hopper, the stresses in the bulk solid are represented by a Mohr's circle that is tangent to the material's effective yield locus. The intersections of the Mohr's circle and the horizontal axis gives the principal stresses. In mass flow, the material is also slipping along the hopper wall, and therefore, the wall stress  $\sigma'$  is represented by the wall yield locus. The shear and normal stresses at the wall are therefore located at the upper intersection of the wall yield locus and the Mohr's circle. The relationship between  $\sigma_1$ ,  $\delta$ ,  $\sigma'$ , and  $\phi'$  is illustrated in Figure 37.

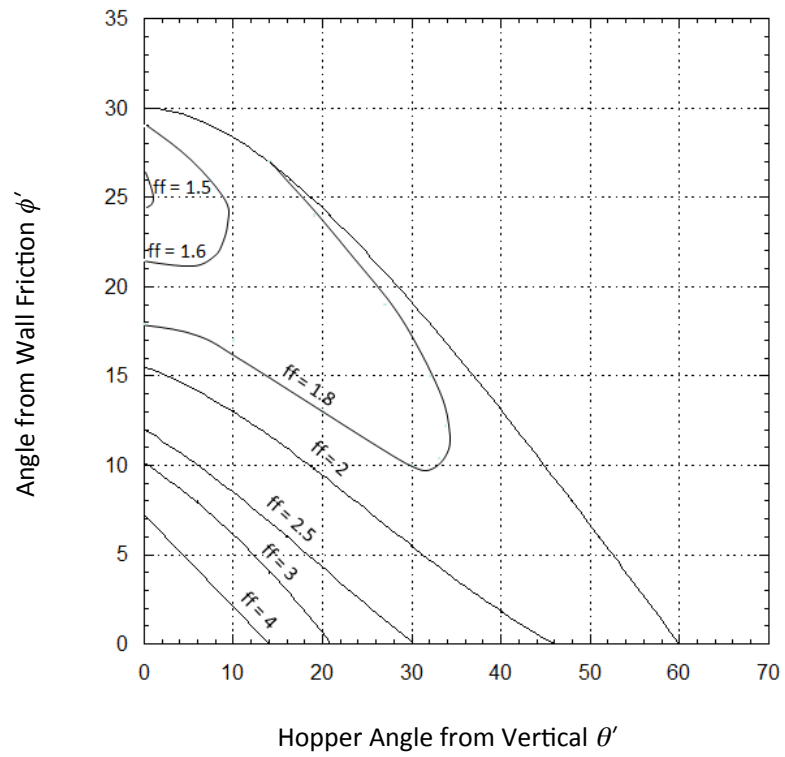


**Figure 29. Flow factors for conical hoppers,  $\delta = 30^\circ$ .**

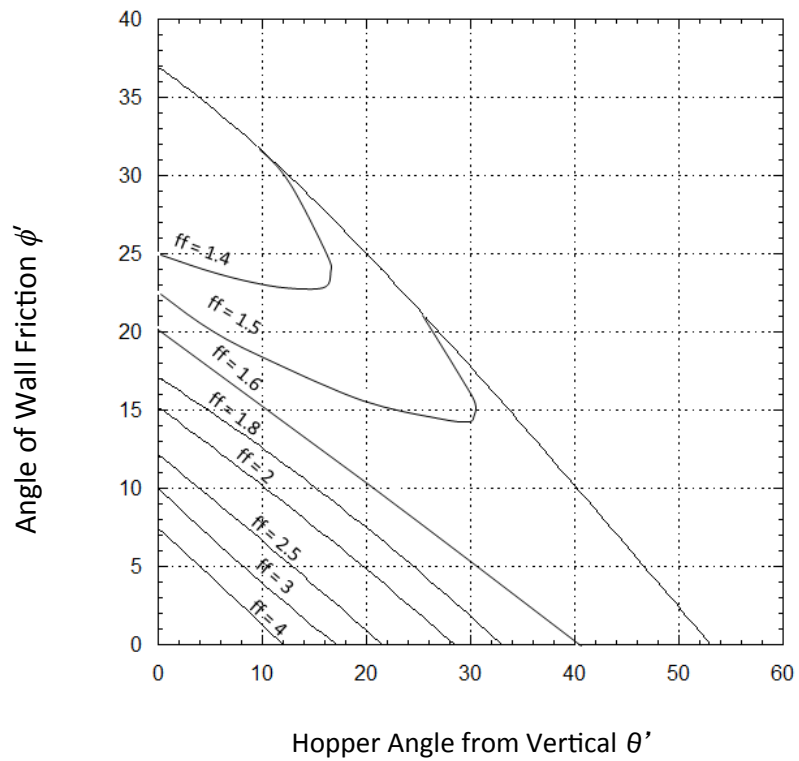


**Figure 30. Flow factors for conical hoppers,  $\delta = 40^\circ$ .**

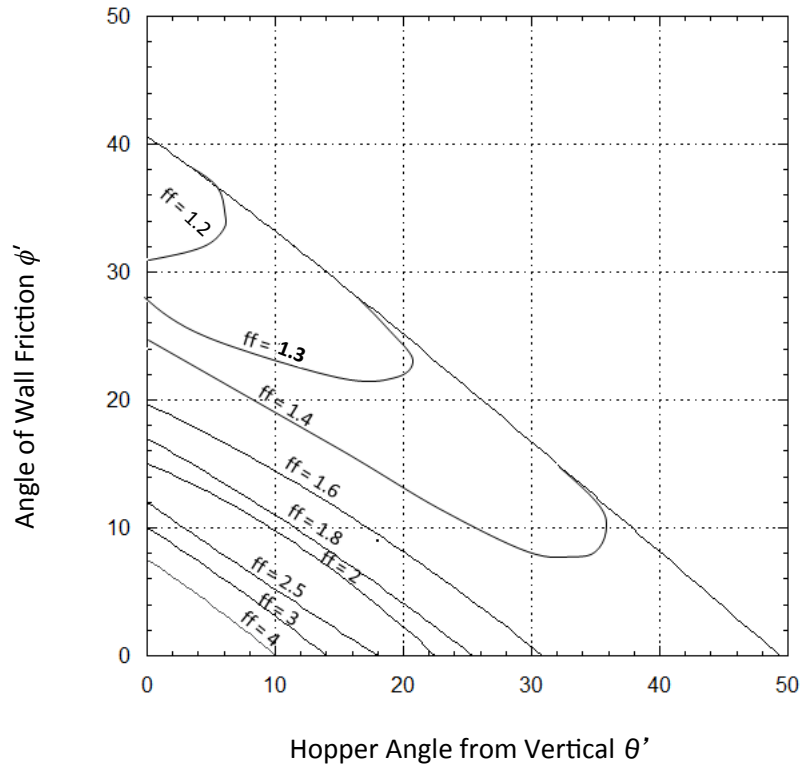


Figure 31. Flow factors for conical hoppers,  $\delta = 50^\circ$ .

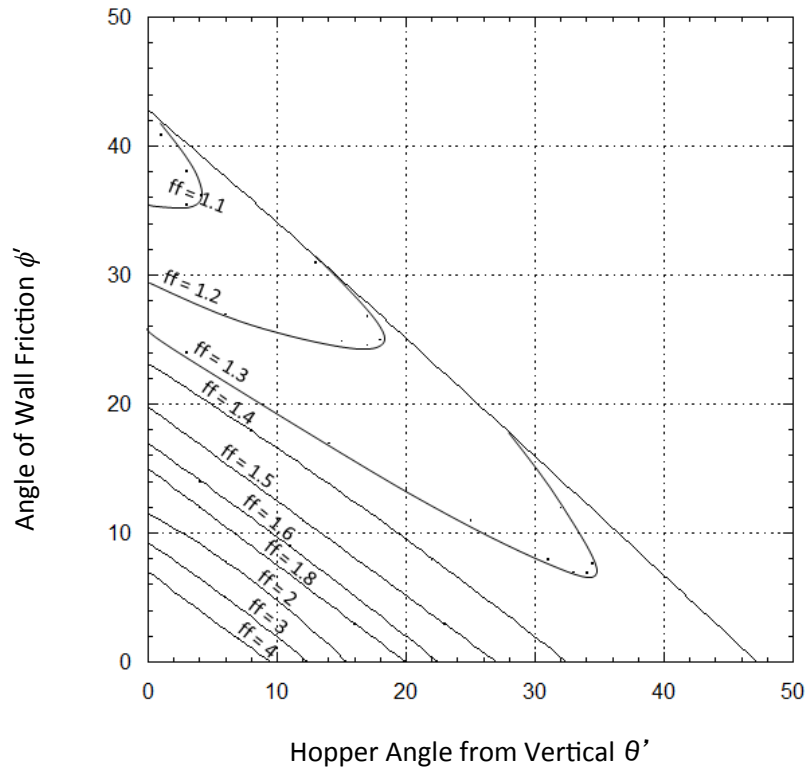


Figure 32. Flow factors for conical hoppers,  $\delta = 60^\circ$ .

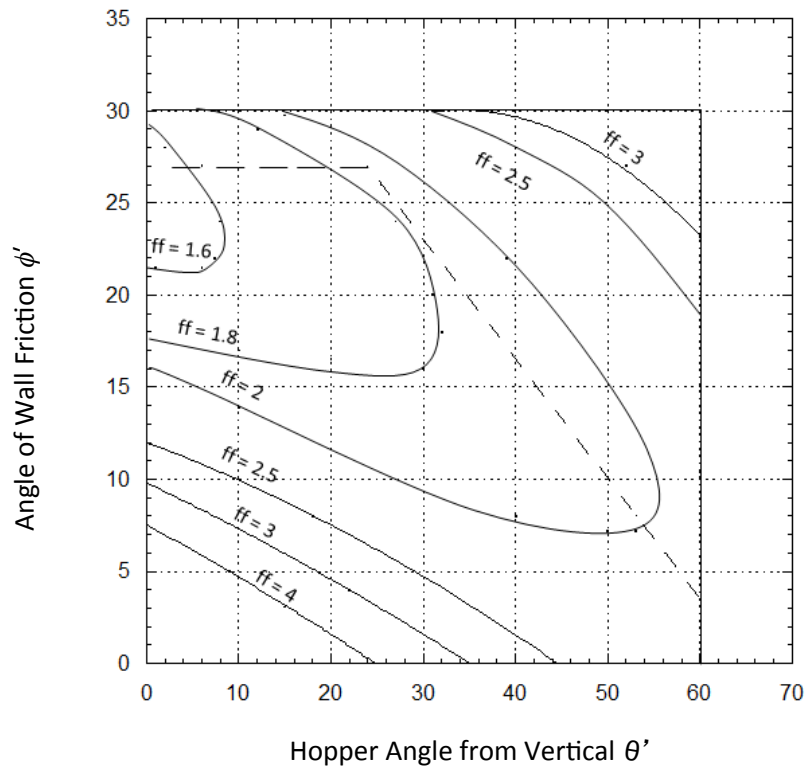


Figure 33. Flow factors for planar flow hoppers with slotted outlets,  $\delta = 30^\circ$ .

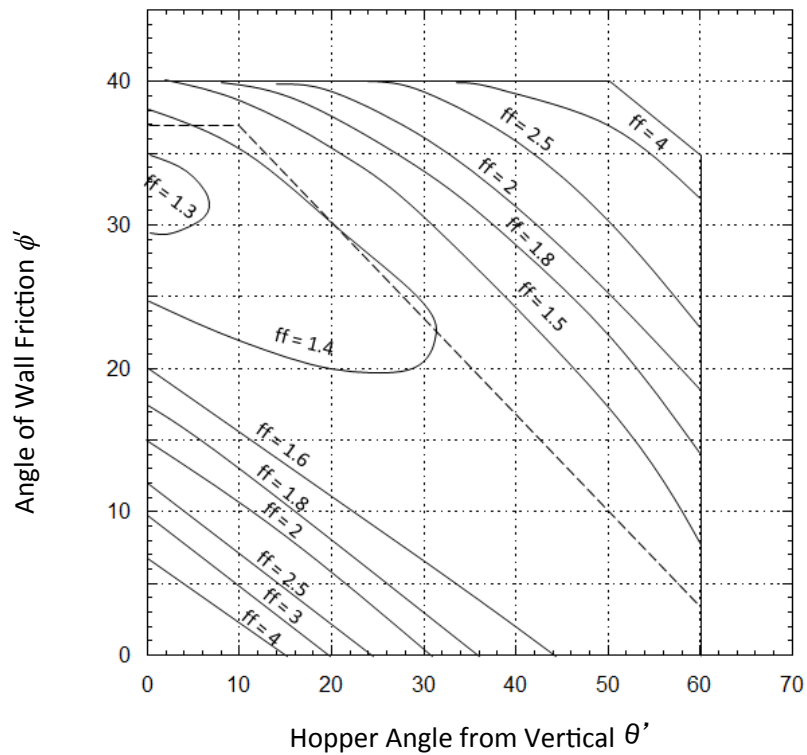


Figure 34. Flow factors for planar flow hoppers with slotted outlets,  $\delta = 40^\circ$ .



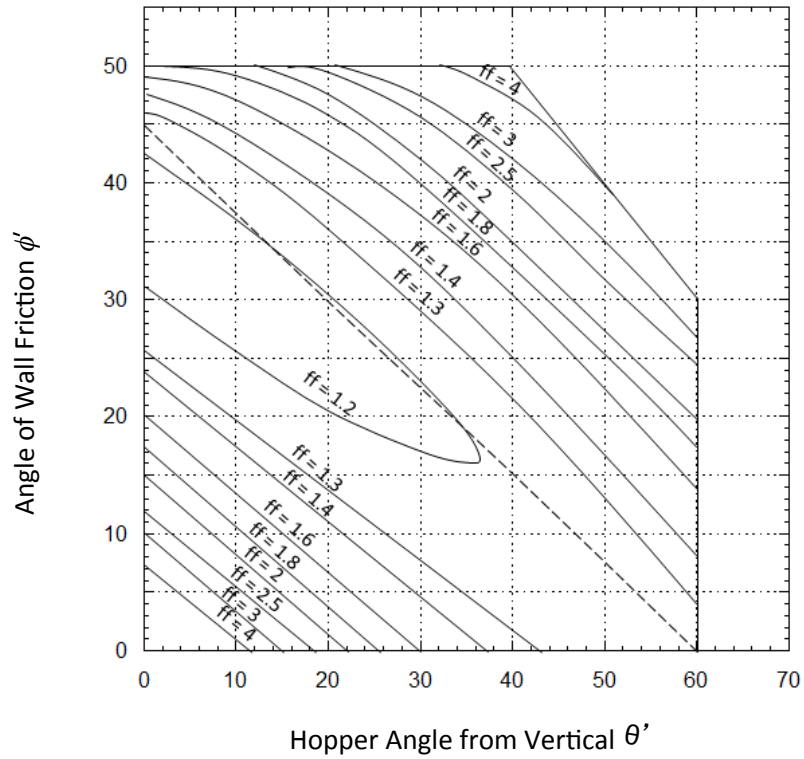


Figure 35. Flow factors for planar flow hoppers with slotted outlets,  $\delta = 50^\circ$ .

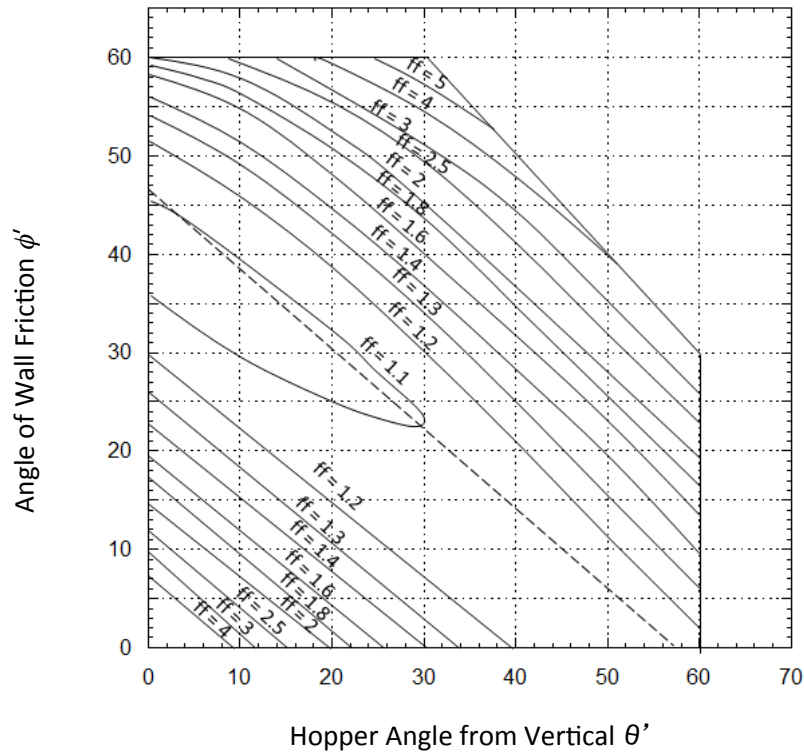
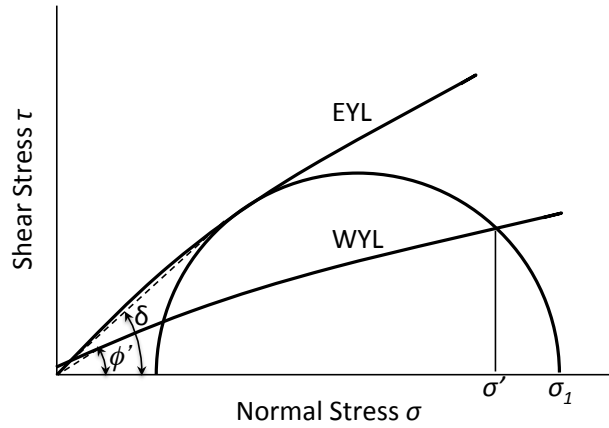


Figure 36. Flow factors for planar flow hoppers with slotted outlets,  $\delta = 60^\circ$ .



**Figure 37. Construction of effective yield locus and wall yield locus.**

To determine the size of the outlet required to prevent arching, the Flow Function and flow factor are compared. The flow factor is dependent on the material's effective angle of friction  $\delta$  and its angle of wall friction  $\phi'$ , as well as the hopper angle and geometry. The angle of wall friction is a function of the stress normal to the hopper wall  $\sigma'$ . Hence, unless the angle of wall friction and effective angle of friction are constant, calculation of the critical outlet diameter or width is iterative. The procedure is as follows [Jenike, 1964]:

1. The effective angle of friction  $\delta$ , wall friction angle  $\phi'$ , and bulk density  $\rho_b$  are estimated.
2. The hopper angle is selected, one that ensures mass flow, by using the appropriate charts (Figure 23 or Figure 24). Note that if a conical hopper is to be specified, a safety factor of at least  $3^\circ$  should be used with respect to the theoretical mass flow boundary.
3. The flow factor  $ff$  is determined from the appropriate chart given by Figures 29 through 36.
4. The flow factor and Flow Function are plotted together. As shown in Figure 38, there are three possibilities:
  - a. There is no intersection, and the Flow Function lies below the flow factor. A dimension  $B$  that is the minimum that prevents cohesive arching cannot be determined. Instead,  $B$  is selected based on other considerations such as discharge rate requirements, choice of feeder, or prevention of particle interlocking. The major consolidation stress  $\sigma_1$  is determined from Equation 41:

$$\sigma_1 = ff \frac{\rho_b g B}{H(\theta')} \quad (41)$$

- b. The flow factor and Flow Function intersect. The minimum outlet dimension  $B_{min}$  is calculated using Equation 42:

$$B_{min} = \frac{H(\theta') \sigma_{crit}}{\rho_b g} \quad (42)$$

- Larger outlet diameters or widths of course can be used, and they are generally selected by considering standard feeder sizes or discharge rate requirements.
- c. There is no intersection and the Flow Factor lies above the flow factor. Gravity flow will no longer be possible in a hopper with converging walls. Consideration should be given to changing the flow properties of the material, such as increasing its particle size, reducing its moisture content, or using a flow aid.
  5. The value of  $\phi'$  at the outlet is checked. The effective angle of friction is determined from a plot of  $\delta$  against  $\sigma_1$ , and the effective yield locus is drawn by drawing a straight line through the origin at an angle equal to  $\delta$ . A Mohr's circle is drawn through  $\sigma_1$  that is tangent to the effective yield locus. The value of  $\phi'$  is found from the intersection of the Mohr's circle and the wall yield locus, as shown in Figure 37.
  6. The recommended hopper angle  $\theta'$  is updated based on the new value of  $\phi'$ . The steps are repeated until convergence is reached.

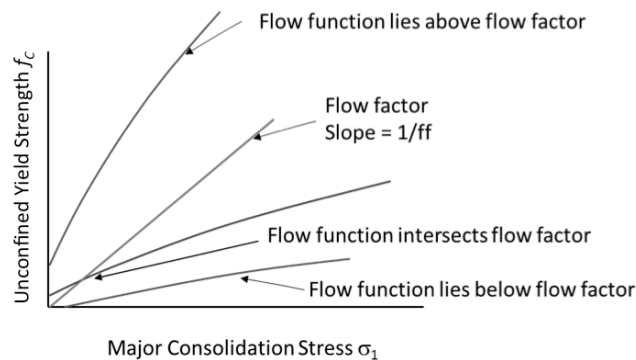


**Figure 38. Plot showing both flow factor and Flow Function.**

To prevent mechanical interlocking the following rules of thumbs are used: for a conical hopper, the outlet diameter should be at least 6-8 times the size of the largest particle that will be handled; for hoppers with slotted outlets, the outlet width should be at least 3-4 times the largest particle size.

If a bulk solid is to be stored at rest in a bin, the Flow Function and wall yield locus must be based on time tests. The intersection of the time Flow Function and flow factor is used to determine the critical stress and hence the minimum outlet size.

### Mass flow discharge rates

While an outlet diameter greater than the minimum will prevent cohesive arching, it may not necessarily be large enough to allow the desired discharge rate. From a force balance together with continuity of the solids, the following equation is derived for the discharge rate of coarse powders from mass flow hoppers:

$$\dot{m}_s = \rho_{b0} A_0 \sqrt{\frac{Bg}{2(m+1) \tan \theta'}} \quad (43)$$

where  $\dot{m}_s$  is the solids discharge rate,  $A_o$  is the cross-sectional area of the outlet,  $\rho_{bo}$  is the bulk density of the material at the hopper outlet,  $m$  is equal to 1 for conical hoppers and equal to 0 for hoppers with straight walls and slotted outlets, and  $B$  is the diameter of the outlet of a conical hopper or the width of a slotted outlet beneath a planar flow hopper.

The maximum flow rate of a fine powder can be several orders of magnitude lower than that of coarser materials. Two-phase flow effects are significant due to the movement of interstitial gas as the powder compresses and expands during flow. Figure 39 illustrates solids and gas pressure profiles in bins for coarse (high permeability) and fine (low permeability) powders.

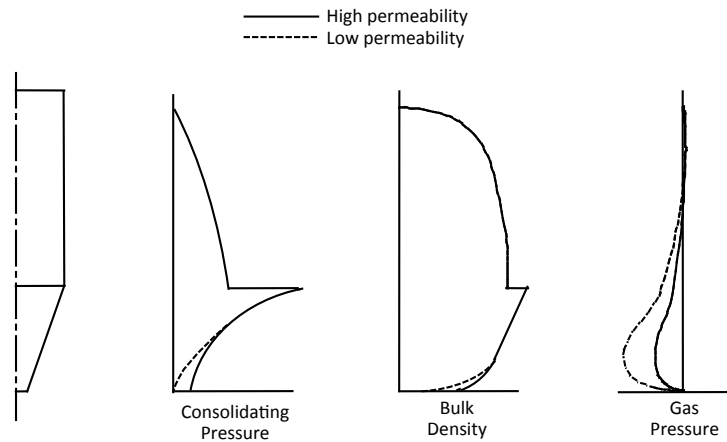


**Figure 39. Consolidating pressure, bulk density, and gas pressure profiles for (high permeability) and fine (low permeability) powders.**

In the cylindrical portion of a bin, the stress level increases with depth, causing the bulk density of the material to increase and the void fraction to decrease, squeezing out a portion of the interstitial gas. This gas leaves the top free surface of the bulk material. In the converging section of the vessel, the consolidated material expands as it moves toward the outlet, reducing the material's bulk density and increasing its void fraction. This expansion results in a reduction in interstitial gas pressure to below atmospheric (*i.e.*, vacuum), causing gas counter flow through the outlet if the gas pressure below the outlet is atmospheric. At a critical solids discharge rate, the solids stress drops to zero, and efforts to exceed this limiting discharge rate will result in erratic flow.

For fine powders, the discharge rate from a mass flow hopper is given by:

$$\dot{m}_s = \rho_{bo} A_o \sqrt{\frac{Bg}{2(m+1)\tan\theta'} \left( 1 + \frac{1}{\rho_b g} \frac{dP}{dz} \Big|_o \right)} \quad (44)$$

Because the gas pressure gradient at the outlet  $dP/dz|_o$  is often less than zero for fine powders, Equation 44 shows they can have discharge rates dramatically lower than those of coarse powders.

The gas pressure gradient is related to the material's permeability and the rate of air counterflow by Darcy's law (Equation 30). Gu *et al.* [*Powder Techn.*, 72, 39 (1992)] derived a relationship between the air and solids flow rates that when combined with Darcy's law gives:

$$\left. \frac{dP}{dz} \right|_O = \frac{\dot{m}_s \rho_{bO} g}{K_O A_O} \left( \frac{1}{\rho_{ba}} - \frac{1}{\rho_{bO}} \right) \quad (45)$$

where  $K_O$  is the permeability of the powder at the hopper outlet,  $\rho_{bO}$  is its bulk density at the outlet, and  $\rho_{ba}$  is the bulk density at a location inside the hopper where the gas pressure gradient is equal to zero. Calculating this value is challenging, and therefore an estimate that is proportional to the stress given by the Janssen equation is frequently used. Note that the calculated limiting mass flow discharge rate can be very sensitive to the choice of  $\rho_{ba}$ .

The stress balance used in the analysis does not account for the cohesiveness of the powder, and hence the expressions are only valid for outlet sizes that are significantly larger than the critical arching dimensions. Jenike & Johanson, Inc. (Tyngsboro, Massachusetts, USA) uses a proprietary computer model based on unconfined yield strength, permeability and compressibility data to calculate discharge rates from mass flow bins.

To increase the flow rate of fine powders, injection of a small amount of air above the hopper outlet is often effective, as it will eliminate the opposing air pressure gradient if injected at the correct rate and at the proper location.

### **Funnel flow outlet size to prevent arching and ratholing**

For funnel flow hoppers, the outlet must be large enough to prevent both a cohesive arch and stable rathole from developing. The critical rathole diameter is calculated by first determining the major consolidating pressure,  $\sigma_1$ , on the bulk solid. The consolidating load can be estimated by the Janssen equation:

$$\sigma_1 = \frac{\rho_b g R_H}{k \tan \phi'} \left[ 1 - \exp \left( \frac{-k(\tan \phi') h}{R_H} \right) \right] \quad (46)$$

where  $R_H$  is the hydraulic radius of the vertical section of the hopper,  $h$  is its height, and  $k$  is the Janssen coefficient.

Jenike [1961] calculated the stress on a rathole as

$$\bar{\sigma}_1 = \frac{\rho_b g D}{G(\phi_t)} \quad (47)$$

where  $D$  is the diameter of a round outlet or the diagonal of a slotted outlet and  $G(\phi_t)$  is a function given by Jenike, which is plotted in Figure 40. Using Jenike's flow/no flow postulate, the rathole will collapse provided that the flow channel stress is greater than the cohesive strength of the bulk solid that makes up the rathole. The critical rathole diameter  $D_F$  can therefore be calculated as:

$$D_F = \frac{G(\phi_t) f_C}{\rho_b g} \quad (48)$$

where  $f_c$  is the unconfined yield strength of the bulk solid at the consolidation pressure given by the Janssen equation.

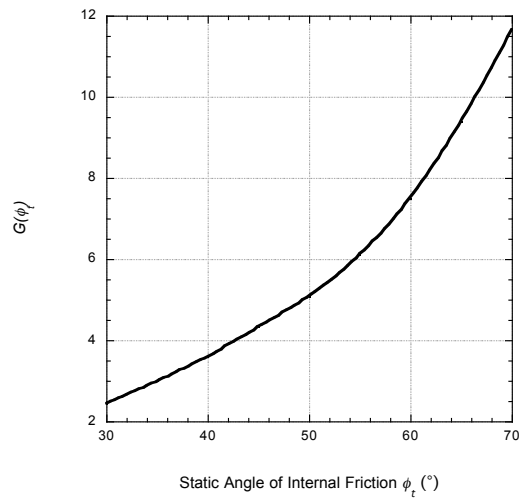


**Figure 40. Function  $G(\phi)$**

A conical funnel flow hopper with an outlet diameter smaller than  $D_F$  or a planar funnel flow hopper with an outlet whose diagonal is less than  $D_F$  will not empty completely. This is illustrated in Figure 41. Because the major consolidation stress is higher in the lower part of the bin, the unconfined yield strength of the bulk solid will be correspondingly higher. As material discharges in a funnel flow pattern, ratholes that form in the upper part of the vessel may continually collapse, provided that the stress on the stagnant material is greater than its cohesive strength. However, if the size of the outlet is smaller than the critical rathole diameter, a level will be reached where the ratholes will no longer fail.

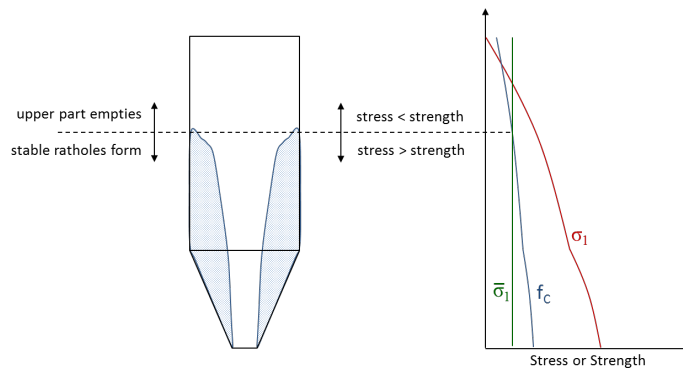


**Figure 41. Formation of a stable rathole in a funnel flow hopper.**

If a hopper with a square or round outlet is designed with an opening large enough to prevent development of a stable rathole, cohesive arching will not occur. When funnel flow hoppers with elongated outlets are designed, prevention of arching must also be considered, *i.e.*, the width of the slotted outlet must be large enough to prevent a cohesive arch from developing. The same procedure that is used to determine the minimum outlet width to prevent arching in a planar flow mass flow hopper is followed, except that a flow factor of 1.7 is used.

### Expanded flow hopper dimensions

An expanded flow hopper is essentially a funnel flow hopper above a mass flow hopper. The upper diameter of the mass flow section must be larger than the critical rathole diameter  $D_F$ , while its outlet size must be larger than the critical arching dimension. An example of an expanded flow hopper is shown in Figure 42.

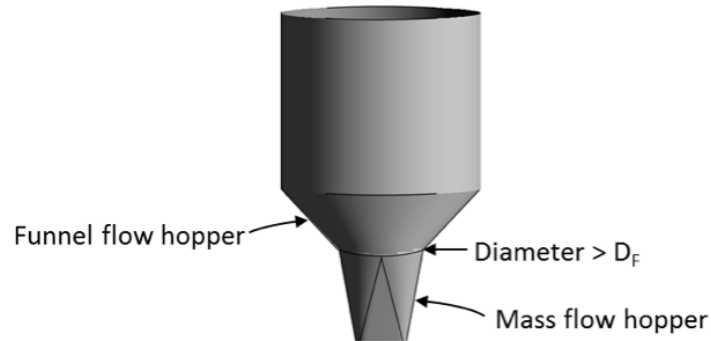


**Figure 42. Expanded flow hopper.**

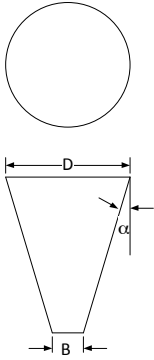
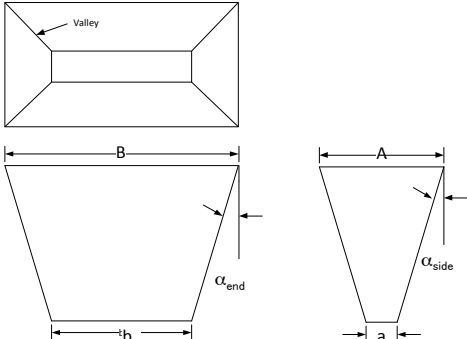
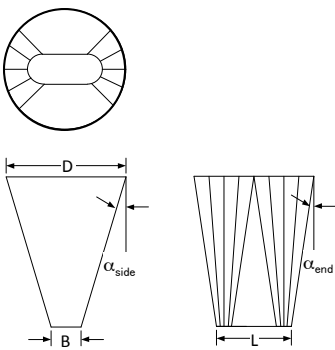
The main advantage of expanded flow compared to complete mass flow is that the overall bin height is less while at the same time a stable rathole cannot develop.

### Capacity

The mass of bulk material that must be stored is generally based on production rate, frequency of operation, required inventory, and in some cases, residence time. Once the required mass has been determined, the necessary volumetric capacity can be determined. Because bulk solids are generally compressible, a suitable average bulk density should be used when converting mass to volume. To be conservative, a low bulk density value should be chosen to ensure that the volume of the bin is sufficient. Also note that the working capacity of a bin will be less than the actual volume since a pile will form when the bin is filled.

A reasonable height-to-diameter ratio ( $H/D$ ) of the cylinder section should be used, with ratios between about 1.5 to 4 usually being the most economical. Height may be limited because of building constraints, zoning considerations, or constraints imposed by other structures or equipment.

The volume  $V$  and height  $H$  of some common hopper designs are given in Figure 43.

<p style="text-align: center;"><b>Conical</b></p> 	$H = \frac{D - B}{2 \tan \alpha}$ $V = \frac{\pi(D^3 - B^3)}{24 \tan \alpha}$
<p style="text-align: center;"><b>Pyramidal</b></p> 	$H = \frac{A - a}{2 \tan \alpha_{side}} = \frac{B - b}{2 \tan \alpha_{end}}$ $V = \frac{H[2(AB + ab) + Ab + aB]}{6}$
<p style="text-align: center;"><b>Transition</b></p> 	$H = \frac{D - B}{2 \tan \alpha_{side}} = \frac{D - L}{2 \tan \alpha_{end}}$ $V \approx \left[ \frac{\pi D^2}{12} + \frac{BL}{3} + \frac{D(B + 2L)}{12} \right] H$

**Figure 43. Hopper capacities.**

The location and number of inlets to a bin is not as important as the number and location of its outlets. In general, the use of a single outlet is preferable. If multiple outlets are required, the best option is to use a single, centered outlet beneath the hopper section and then splitting the stream beneath it.



If multiple outlets are to be located below a circular cylinder, each outlet should be located equidistantly from the bin centerline. Examples of proper and improper multiple outlet designs are shown in Figure 44. If a bin is center-filled, the outlet arrangement on the right is preferable to that on the left because similar material discharges from each outlet provided that all outlets are fully open and material is discharging at approximately the same rate from each one.

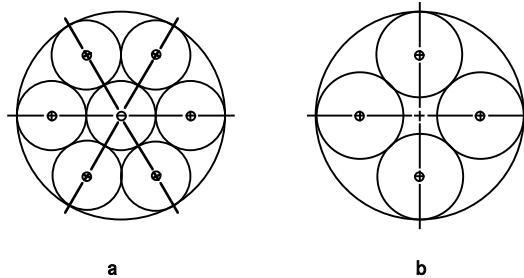


**Figure 44. Multiple outlets below a circular cylinder; (a) poor design; (b) recommended design.**

### Useful guidelines

The quality of construction of a bin – particularly its interior surface -- is critical to its ability to function as desired. If horizontal welds, incorrectly lapped liner plates, or poorly constructed mating flanges exist in a bin designed for mass flow, it may discharge in a funnel flow pattern. The lower of two mating flanges should be oversized to prevent any protrusions into the flowing solid. All flanges should be attached to the outside of the hopper, with the hopper wall material being the surface in contact with the flowing solids.

A feeder, slide gate, or both may be used below the hopper outlet. If a gate is used below a mass flow hopper, the gate must be either fully open or fully closed. A partially opened gate creates a flow obstruction and will convert what would otherwise be a mass flow design into funnel flow. A gate should never be used to modulate flow in a mass flow bin.

When using a feeder under a slotted outlet, its capacity must increase along the outlet length in the discharge direction. This is generally accomplished using a specially designed screw or belt. When a screw feeder is used, the screw should be comprised of a section having a tapered shaft and a constant shaft diameter, increasing pitch section. A properly designed interface between a slotted outlet of a hopper and a belt will progressively discharge more material onto the belt along its length.

A rotary valve is often used as a feeder under a conical hopper outlet to control flow. Common problems experienced with such use of a rotary valve are arching of material over the valve opening, erratic discharge, and preferential flow from one side of the hopper into one side of the valve. Most rotary valves have a transitioning throat area, which is significantly smaller than the nominal size of the valve and may be too small to prevent arching. In addition, this transition section may have a rougher than expected surface preventing flow along it. Preferential flow can be overcome by having a vertical section with a length greater than its diameter.

Gas leakage through the rotary valve often restricts the material discharge rate, thereby lowering the efficiency of the valve and can even cause arching and erratic discharge. Proper venting of rotary valves is usually important, but it is critical if a fine powder is being handled.

Handling an abrasive bulk solid in a mass flow bin may result in significant abrasive wear of the wall material. Generally, the hopper surface becomes smoother with wear; however, occasionally the wall becomes rougher, which may upset mass flow. Wear is a function of the bulk solid flow properties, wall surface, solids pressure, and velocity. The life of a given wall material can be estimated by conducting wear tests in which a screw continuously feeds a fresh sample of bulk solid to a rotating coupon of wall material.

The material of construction of most bins is metal, with reinforced concrete the most common alternative. When because of its size the bin must be erected in the field, reinforced concrete should be considered. A double layer of reinforcing steel (rebar) is likely required, especially if eccentric loads are possible. Reinforced concrete is also preferred over metal if abrasion or corrosion is a concern.

### **Flow aids**

Flow aids are mechanical or pneumatic devices or chemical additives used to induce bulk solids to flow more easily. Vibrators and air cannons are two examples of common mechanical and pneumatic flow aids. Common chemical additives include silicates, stearates, and phosphates.

Vibrators impart forces to the bulk solid through the walls of the storage vessel, most frequently on the hopper walls. Some vibrators produce low-frequency, high-amplitude forces, while others deliver high-frequency, low-amplitude forces. Their effect on flow obstructions can vary. In some cases, they may be an effective means of restoring flow when a bin becomes plugged. In many cases, however, their effect is minimal or can even exacerbate flow problems. Applying sufficient but not excessive force where it is required to collapse an arch or rathole is difficult, particularly in the case of a rathole where the force must usually be transmitted through a significant mass of material to reach it.

The force required to overcome a cohesive arch depends on the bulk solid's cohesive strength and the size of the outlet. If the hopper outlet is slightly undersized, that is, its diameter or width is only marginally smaller than its critical arching dimension after storage at rest, a vibrator may be able to provide enough energy to restart flow. Because ratholes are inherently stable, the outlet diameter required to prevent a rathole from forming can be several times the outlet size of a bin; thus vibrators in general cannot be used to overcome ratholing.

A steep Flow Function is evidence of a bulk solid that is pressure sensitive, *i.e.*, its strength increases substantially when additional stresses are applied. Vibrating such a bulk solid often makes flow problems more severe.

A vibrating discharger or bin activator employs an inverted cone or dish that moves in a gyratory, horizontal, or vertical motion. The bulk solid then flows around the cone or dish into a conical section below it, which essentially operates as a chute. Vibratory dischargers can be effective in

overcoming flow problems in some bins provided that they are used appropriately. When used at the outlet of a funnel flow bin, the flow channel above it will be approximately the size of the top diameter of the discharger. If this diameter is smaller than the material's critical rathole diameter, a stable rathole will form, and the discharger will be ineffective in overcoming it.

Air (or nitrogen) cannons operate differently in that they rely on a pressure wave to provide the stress required to break an arch. Cannons work by releasing a volume of high-pressure gas into the bin. The required size, number, and location of the cannons depend on the cohesive strength of the bulk material and the dimensions of the bin.

Air cannons are best used for reinitiating flow after a cohesive arch develops when the material is stored at rest. If flow problems occur without storage at rest, air cannons are unlikely to be a viable solution, as they must be fired repeatedly to maintain flow. Air cannons are usually not effective in preventing flow problems in funnel flow bins since ratholes are inherently stable.

Chemical flow aids are often used to prevent arching or the formation of a stable rathole. Parting agents such as silicates, stearates, and phosphates are effective as they increase the distance between adjacent particles, thereby reducing the magnitude of their cohesive forces. Note that while a flow aid may be effective in reducing a bulk solid's cohesive strength, the additive may increase wall friction, potentially resulting in flow problems associated with funnel flow.

### **Inserts**

A disadvantage of mass flow bins is that relatively steep hopper sections are generally required, so in some cases bins may be too tall for the available space. When properly designed, an insert can be used to allow mass flow in a bin with shallow hopper walls that, without modifications, would discharge in a funnel flow pattern.

Cone-in-cone and bullet designs are shown in Figure 44. The cone-in-cone insert, or Binsert<sup>®</sup>, is designed to allow mass flow through the inner cone and also through the annular space between the inner and outer cones. The angle of the inner cone is equal to or steeper than the hopper angle recommended for mass flow in a conical hopper, and the angle of the outer cone is equal to double that of the inner cone. The outlet diameter of the inner cone must be greater than the critical arching diameter. For cohesive materials that would otherwise arch over the outlet of the inner cone of an insert, an inverted cone or "bullet" can be placed above the inner cone.

---

<sup>®</sup> Binsert is a registered trademark of Jenike & Johanson, Inc.

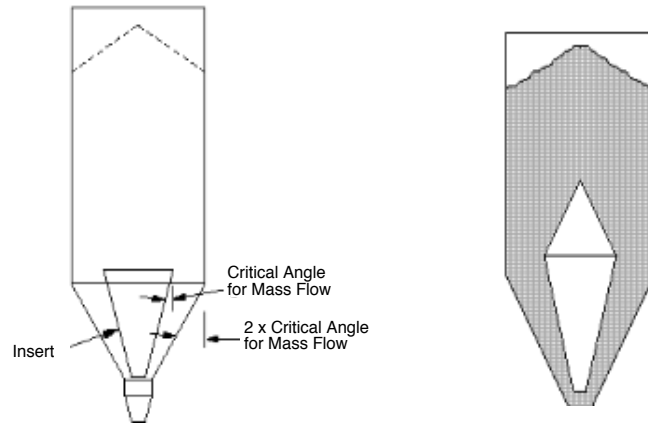


**Figure 44. Inserts; cone-in-cone, left, and bullet, right.**

Note that the location of the inner cone and, when applicable, the size of the bullet greatly influence the effectiveness of an insert. An insert that is too high or too low relative to its optimum size and position will expand the flow channel very little, if at all. Also note that the loads acting on inserts are usually very high, and therefore the supports required to resist these loads may be large and can impede flow.

### **Air assist and fluidization**

Air pads and air nozzles are sometimes used to inject low-pressure air into a bin. While they are generally ineffective in correcting problems caused by arching or ratholing, they may be useful in increasing the discharge rate of fine powders by reducing the adverse pressure gradient that develops above a hopper outlet and the resulting counterflow of air.

A better technique to increase the discharge rate of fine powders is to use an air permeation system, which consists of a sloping shelf or insert through which a relatively low flow rate of air is introduced. The air reduces or eliminates the vacuum that naturally develops when a bulk solid dilates in the hopper section, increasing its void fraction. To be effective, the air should be distributed uniformly, its flow rate should be low enough to prevent fluidization, and the permeation system should not impede solids flow in the hopper.

Air-assist dischargers are designed to reduce the wall friction angle to nearly zero, thereby allowing powders to flow along hopper walls. The hopper section is either lined with air panels or is fabricated using a permeable membrane through which a small amount of air is injected. Jenike [1964] recommends conical hopper angles between  $40^\circ$  and  $50^\circ$  from vertical as steeper hoppers may require large outlet diameters to prevent arching. Shallow hopper angles can be used provided that a fully open, unrestricted on/off valve is used or if enough gas is added to completely fluidize the bulk material, *i.e.*, a fluidized discharger is used.

A fluidized discharger can be used when the bulk material is fluidizable and a low bulk density of the discharged material is acceptable. Fluidized dischargers can generally be used for Geldart Group A, B, and C materials [*Powder technology*, 7, 5 285 (1973)], although Group C materials may

require mechanical agitation. Discharge from a bin equipped with a fluidized discharger is typically controlled through use of a rotary valve.

### Standpipes

A standpipe is frequently used to seal a bin outlet against gas pressures. It is composed of a vertical cylinder mounted between the bin and feeder. Its major advantages over other methods such as sealing screws is that it has no moving parts and it is inexpensive to fabricate and operate.

A standpipe provides a seal against gas pressure by providing a sufficient length to lower the pressure gradient such that the flow of gas through the bed of solids at the hopper outlet is reduced to an acceptable rate. Standpipe design is discussed by Carson and Marinelli [*Power Engr.*, 85, 11 (1981)].

### Chutes

Chutes are used to direct the flow of bulk solids. They need to be properly designed to avoid problems such as plugging, excessive wear, dust generation, and particle attrition.

A chute must be sufficiently steep and low enough in friction to permit sliding and clean off. Referring to Figure 45, the velocity of a stream of particles (assuming no bouncing) after impacting a chute,  $V_2$ , relative to its velocity before impact,  $V_1$  is:

$$V_2 = V_1(\cos \theta - \sin \theta \tan \phi') \quad (49)$$

where  $\theta$  is the impact angle and  $\phi'$  is the wall friction angle.

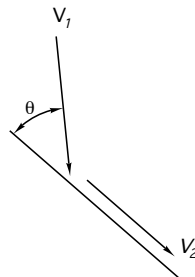


**Figure 45. Velocity of a particle after impact on a chute.**

If the particles fall freely when they are dropped onto the chute, their velocity before impact  $V_1$  is given by:

$$V_1 = \sqrt{2gH} \quad (50)$$

where  $H$  is the drop height.

If the sum of  $\phi'$  and  $\theta$  equals  $90^\circ$ ,  $V_2$  will be reduced to zero, and the bulk material will not slide on the chute surface unless its angle of inclination is greater than a minimum value. To determine this minimum value required to overcome adhesion at impact, chute tests [*Bulk Solids Handling*, 12, 3, 447 (1992)] can be performed. A sample of the bulk material is loaded onto a wall coupon and a load representing the impact pressure is briefly applied. The impact pressure  $\sigma$  is given by:

$$\sigma \approx \rho_b V_1^2 \sin^2 \theta \quad (51)$$

The coupon is inclined about a pivot point until it just starts to slide. Usually a safety factor of 5° is applied to this minimum value to ensure clean off.

While sliding on a straight surface, the particles will accelerate or decelerate, depending on the relative values of the chute angle  $\alpha$  measured from horizontal and the wall friction angle  $\phi'$  (see Figure 46):

$$a = g(\sin \alpha - \cos \alpha \tan \phi') \quad (52)$$

where  $a$  is the acceleration.

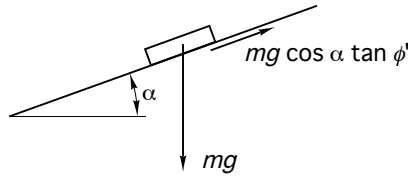


**Figure 46. Element of bulk solid sliding on a straight chute.**

Assuming that the chute cross section does not decrease along a distance  $S$  on the chute surface, the stream velocity  $V$  is given by:

$$V = \sqrt{V_0^2 + 2aS} \quad (53)$$

where  $V_0$  is its velocity at the starting point.

When the velocity of the stream changes as it passes through a chute, its cross-sectional area will change. To prevent flow stoppages, the chute should be sized such that it is no more than about one-third full at the point of minimum velocity.

While chutes can be fabricated and installed in rectangular sections, having curved surfaces upon which the material slides has advantages. Chutes composed of cylindrical pipes or rounded surfaces control the stream well, as they can be used to center the load allowing the momentum of the material to keep the chute clean. The path that the bulk material will flow depends on its frictional properties and flow rate. Discrete Element Method (DEM) models should be used to design chutes with complicated geometries.

Free fall height and sudden changes in the direction of material flow should be minimized to reduce solids impact pressures, which can result in high abrasive wear, attrition, and generation of dust. Since impact pressure is proportional to  $\sin \theta$  and  $V_1^2$ , reducing the impact angle  $\theta$  and drop height  $H$  will reduce wear, and the momentum of the flowing material will keep the chute surface cleaned off.

Dust is created when air is entrained into the flowing material. To avoid dusting, the chute should be designed such that the material remains in contact with the chute surface, the material stream is concentrated, and the velocity through the chute is kept nearly constant. If the material is to land on

a belt conveyor at the exit of the chute, the velocity of the stream should be in the direction of and equal to or greater than the velocity of the belt.

Attrition of friable particles is most likely to occur at impact points where the impact pressures are high. Therefore, attrition can be minimized by minimizing the impact angle  $\theta$ , ensuring that the flowing stream is concentrated and remains in contact with the chute surface, and maintaining a constant stream velocity.

### Segregation

Some materials, when transferred into a bin, will segregate, that is, particles of different size, shape, density, *etc.* will separate. Segregation can occur by a number of different mechanisms, depending on the physical characteristics of the particles and the method of handling. The three most common mechanisms are *fluidization* (air entrainment), *dusting* (particle entrainment), and *sifting*. These segregation methods are illustrated in Figure 47.

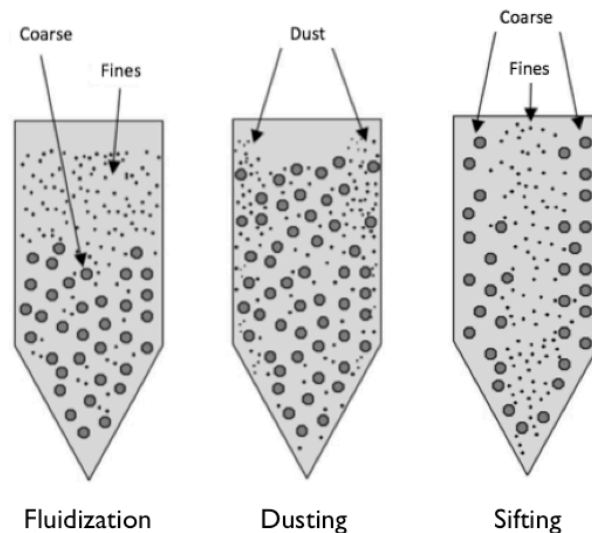


**Figure 47. Segregation by fluidization, dusting, and sifting.**

Fluidization, or air entrainment, can cause vertical segregation, *i.e.*, horizontal layers of fines and coarse material. Fine powders generally have a lower permeability than coarse materials and therefore retain air longer. Thus, when a bin is being filled, the coarse particles are driven into the bed while the fine particles remain fluidized near the surface. Air entrainment often develops in materials that contain a significant percentage of particles below 100  $\mu\text{m}$  in size. Fluidization segregation is also likely to occur when a bin is filled or discharged at high rates or if gas counterflow is present. Segregation by the fluidization segregation mechanism is illustrated in Figure 48.

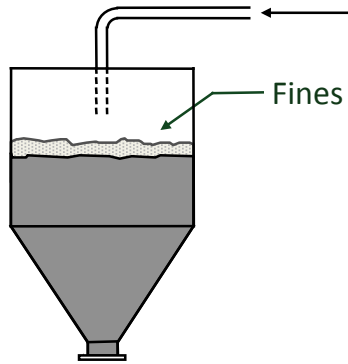


**Figure 48. Segregation due to fluidization of fine, light particles.**

Dusting, or particle entrainment, involves airborne particles, differences in settling velocities between particles, and air currents to cause movement of suspended particles. Dusting can occur when powder is dropped and impacts onto a pile surface, causing the release of finer particles into the air. Particles can also be re-entrained in air if large pockets of air bubble up through a stationary bed of material from below. These particles will tend to remain suspended in the air and be carried by air currents to the least active portion of the receiving vessel's area, generally the lowest part of the pile surface that is furthest away from the impact point. Generally, powders that are susceptible to this mechanism contain a portion of finer particles below 50  $\mu\text{m}$  that do not readily adhere to larger particles. Dusting is illustrated in Figure 49.

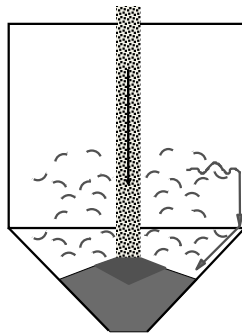


**Figure 49. Particle entrainment during filling of a bin.**

Sifting occurs when smaller particles move through a matrix of larger ones. Four conditions must exist for sifting to occur:

- A difference in particle size between the individual components, typically a minimum ratio of 2:1 or greater.
- A sufficiently large mean particle size, typically one greater than approximately 500  $\mu\text{m}$ .
- Free flowing material.
- Inter-particle motion.

All four of these conditions must exist for sifting segregation to occur. If any one of these conditions does not exist, the mix will not segregate by this mechanism.



Sifting segregation is illustrated in Figure 50, which is a photograph of a typical pile that forms when a vessel is filled. Because coarser particles tend to be more mobile, they roll downward towards the periphery of the pile. Fines percolate through the bed as they fall from the center and accumulate in the middle. The result is side-to-side separation of particles by size.

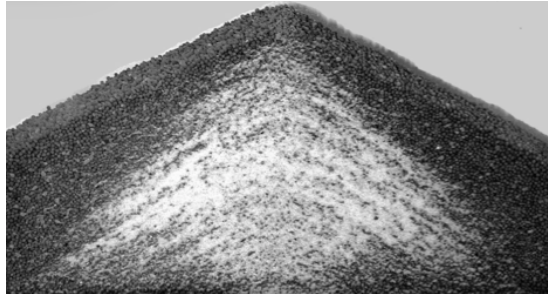


**Figure 50. Sifting segregation after formation of a pile.**

### **Caking**

Caking is frequently moisture-induced. When the moisture content of a bulk material reaches a critical value, moisture will condense primarily at the contact points between adjacent particles, causing liquid bridges. If local drying occurs due to temperature swings during storage or transit, solid bridges may form when soluble components in the liquid precipitate. Water is also a plasticizer for many materials, and its presence can cause particles to deform and increase inter-particle contact area. Elevated temperature and impurities also frequently increase the likelihood of a material to cake.

Caking occurs when the magnitude of inter-particle forces increases significantly over time. These cohesive forces are primarily van der Waals forces, polar interactions, and forces associated with plastic creep or liquid bridges (when moisture is present). van der Waals forces include all intermolecular forces that act between electrically neutral molecules. Polar interactions occur when adjacent particles contain regions that are permanently electron-rich or electron-poor. Van der Waals forces and polar interactions increase as the distance between particles decreases. Although these forces are proportional to particle size, the likelihood of caking generally decreases with increasing particle size since the number of inter-particle contacts is inversely proportional to the square of the particle diameter.

With some bulk materials, plastic creep, which is the tendency of a material to deform when under consolidation, may occur. Plastic creep can be severe if impurities that behave as plasticizers are present or if the bulk solid is subjected to high temperatures for long periods of time, especially when above its glass transition temperature ( $T_g$ ). Differential scanning calorimetry (DSC), thermal mechanical analysis (TMA), and inverse gas chromatography (IGC) are frequently used to measure  $T_g$ . IGC is preferable over the other methods if moisture is known to act as a plasticizer since it can be conducted at a constant relative humidity.

Liquid bridging occurs when moisture accumulates at the contact points between adjacent particles. The likelihood of liquid bridging can often be inferred from a powder's moisture sorption isotherm,

which relates relative humidity and equilibrium moisture content. An example of an isotherm that has the sigmoidal shape characteristic of many bulk materials prone to caking is shown in Figure 49.

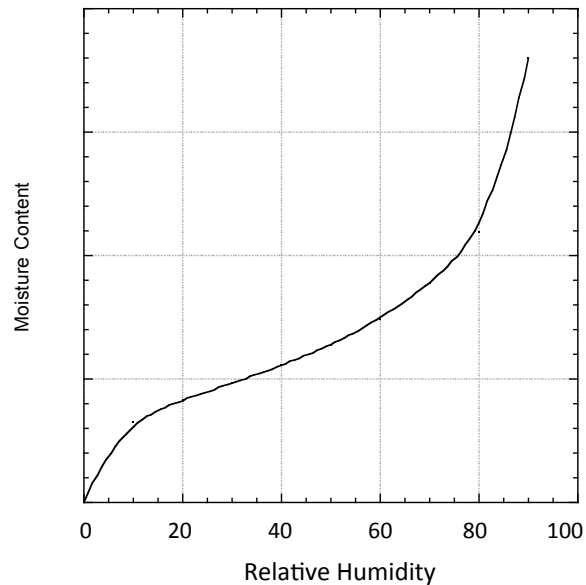


**Figure 49. Example Isotherm**

The moisture isotherm is initially linear as water molecules are adsorbed until a monolayer is formed. The effect of moisture on caking is generally negligible in this region. As relative humidity increases, multilayer adsorption takes place as a consequence of hydrogen bonding. In this region, the slope of the isotherm is initially shallow but steepens with increasing relative humidity. As moisture uptake increases, the particles become surrounded by moisture. If the solids are water soluble, the layer of moisture can be viscous, and the bulk material may become cohesive.

The third region occurs at high relative humidity, where the equilibrium moisture content increases dramatically. In this region, most of the incremental condensation takes place at the contact points between particles. This phenomenon, which is known as capillary condensation, is accompanied by liquid bridging, and it results in strong forces between particles. This leads to caking over time. If soluble matter exists in the liquid bridges, and if the liquid evaporates, then strong, solid bridges may form.

To quantify caking, the temperature, relative humidity, and consolidation pressures used during the test must simulate those expected when the bulk material is stored. A material's unconfined yield strength is best measured using a shear cell tester or uniaxial compression tester. A significant change between the unconfined yield strength measured for continuous handling and after storage at rest indicates that caking has occurred.

Any moisture limits to avoid caking that are based on equilibrium moisture content should account for the possibility of moisture migration. This occurs when a temperature gradient exists during packaging, storage, or transit of powders. The mechanism of caking due to moisture migration is as follows:

- The relative humidity of the interstitial air at the warm boundary decreases.

- As a consequence, moisture desorbs from the warmer solids, as the solids and interstitial air are no longer in equilibrium.
- The *absolute* humidity of the interstitial air increases.
- The driving force in the gas phase leads to moisture migration toward the interior, which has a lower absolute humidity.
- The relative humidity of the cooler interstitial air increases.
- Moisture adsorbs onto solids in the interior in an effort to re-establish equilibrium.

Moisture migration is illustrated Figure 50.

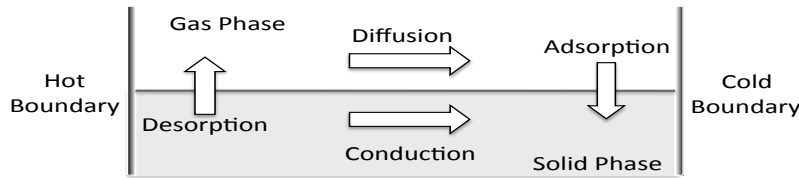


**Figure 50. Schematic describing moisture migration.**

An analysis can be performed to determine the moisture distribution in a bulk solid that will result if a temperature gradient (*e.g.*, if product pack-out temperatures exceed storage temperatures or if storage temperatures vary) is imposed. One assumes that the temperature gradient remains constant. Since this is not true, the analysis results in a conservative view of possible conditions that can exist if temperature differences were to remain for an extended time.

The analysis is as follows. If a bulk solid is exposed to a warm surface (temperature =  $T_H$ ) on one side and a cool surface (temperature =  $T_C$ ) on the other, the temperature profile at steady state would be given by:

$$T = T_C + (T_H - T_C)z \quad (54)$$

where  $z$  is the ratio of the distance from the cold surface to the width between the hot and cold surfaces.

At steady state, the concentration of water in the interstitial air  $C_w$ , is constant. The vapor phase moisture concentration is the product of the absolute humidity  $H$  and the dry air density  $\rho_a$ :

$$C_w = \rho_a H \quad (55)$$

The relative humidity  $RH$  is related to absolute humidity by

$$\frac{RH}{100} = \frac{29HP_t}{(18 + 29H)P_w^{sat}} \quad (56)$$

where  $P_t$  and  $P_w^{sat}$  are the total pressure and saturation pressure of pure water, respectively. Due to the temperature gradient, the relative humidity of the interstitial air will vary. As a result, the amount of condensed moisture that is in equilibrium with the interstitial air will also vary. The relationship between the solid's equilibrium moisture content  $X$  and the relative humidity of the interstitial air is given by the material's isotherm. Since the amount of moisture in the gas phase is

negligible compared to that in the solid, the total amount of moisture in the solid after migration can be assumed to be equal to the initial solid moisture content  $X_0$ , *i.e.*,

$$\bar{X} = \int_z X(z) dz = X_0 \quad (57)$$

A specification for a bulk material's moisture content that, if exceeded, causes caking (as determined from unconfined yield strength measurements) can be determined by finding the value of  $C_w$  that satisfies Equations 55 through 57 and the material's moisture isotherm.

## PROCESS VESSELS

Moving bed process vessels are hoppers, bins, or silos modified to allow processing of a bulk solid. Examples of processes include heating, cooling, conditioning, drying, and conducting a chemical reaction. In some moving bed processors, a gas is injected and passes counter-current or perpendicular to the flow of solids. Others are equipped with plate-and-frame or tubular heat exchangers. Fluidization of the solids is not required, nor is it desired. Rather, the bulk material flows downward as a moving bed towards the processor's outlet.

To ensure trouble-free operation of moving bed processors, the following design criteria must be met:

1. The outlet of the processor must be large enough to prevent solids flow stoppages and to allow the desired production rate.
2. The solids velocity should be as close to uniform across the processor's cross-section as possible and practical. At a minimum, there must not be any regions of stagnant material inside the processor.
3. If required, the gas must be introduced in such a manner that it does not disrupt the flow of solids.
4. The processor must provide the required residence time.
5. If applicable, a driving force for heat or mass transfer must exist throughout the cylindrical section of the processor.

Counter-flow, cross-flow, and radial-flow designs exist (see Figure 51). In a counter-flow system, the gas introduction system must be designed such that there are no regions with high gas velocities as localized fluidization will cause channeling, bypassing of the solids, and flow instabilities. Designs that involve nozzles or perforated plates therefore should be avoided. Gas is most uniform when it is injected into the moving solids bed via an annulus and a set of crossbeams located near the intersection of the cylinder and hopper sections of the processor. Two examples of well-designed gas distributors are shown in Figure 52 [Mehos, *Chem. Engr.* 116, 5, 34 (2009)].

In counter-flow systems, the gas velocity must be low enough to prevent fluidization in the cylindrical section of the processor. A rule of thumb is that the vessel's cross-sectional area at the level of gas introduction should be such that the superficial gas velocity is no more than approximately one-third the bulk material's minimum fluidization velocity.

The gas flow rate must be low enough to prevent excessive entrainment of fines at the top of the column but high enough to ensure that a driving force for mass or heat transfer exists throughout the column if required.

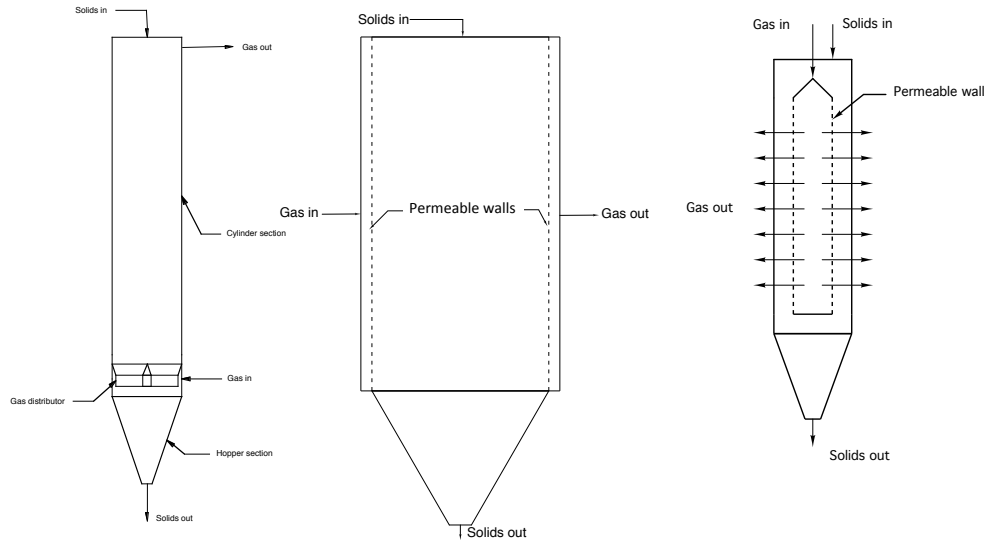


**Figure 51. Process vessels with gas injection – countercurrent (left), cross-flow (center), and radial flow (right).**

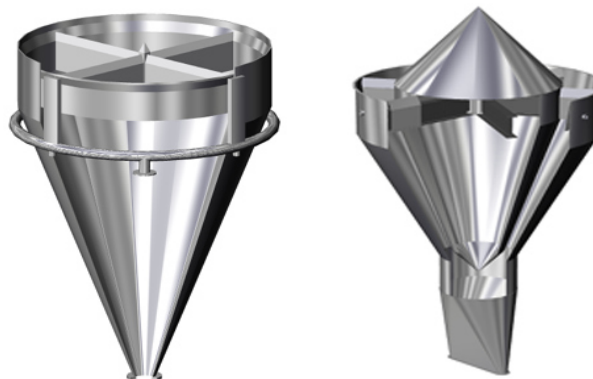


**Figure 52. Gas distributors with crossbeams.**

Cross-flow and radial designs are preferred if the required gas flow rate is high because a low pressure drop will be realized. Cross-flow and radial-flow processors are fabricated with permeable walls through which the gas enters and exits the moving bed of solids.

For cross-flow and radial-flow, the gas velocity must be low enough to prevent pinning or cavity formation. Pinning occurs when the frictional force between the bulk solid and the permeable wall through which the gas exits is great enough to prevent the particles from flowing downward and along the wall. A cavity can develop if the pressure gradient that develops when gas is injected into the bed causes a gap to form between the bulk solid and the wall from which the gas is introduced. If a cavity forms, gas will flow preferably upward rather than across the bed.